The scavenger receptor MARCO is a ligand for the immune inhibitory receptor LAIR-1 and regulates its function in cis

Akashdip Singh[1,2]*, Saskia V. Vijver[1,2]*, Hajar Aglmous-Talibi[1,2]*, Nebojsa Jukic[2,3], Peirong Chen[4], Suzanne Crawley[4], Kalyani Mondal[4], Jing Zhou[4], Christian Niederauer[3], Zimple Matharu[4], Betty Li[4], Bin Fan[4], Michiel van der Vlist[1,2], Daniel D. Kaplan[4], Lee B. Rivera[4], James Sissons[4], Jonathan Sitrin[4], Kristina A. Ganzinger[2,3], M. Ines Pascoal Ramos[1,2,5†], Linde Meyaard[1,2†]

[1]Centre for Translational Immunology, University Medical Centre Utrecht, Utrecht University, Utrecht, the Netherlands.
[2]Oncode Institute, Utrecht, the Netherlands.
[3]Autonomous Matter Department, AMOLF, Amsterdam, The Netherlands.
[4]NGM Biopharmaceuticals Inc, South San Francisco, CA 94080, USA.
[5]Champalimaud Foundation, Champalimaud Centre for the Unknown, Champalimaud Research, Physiology and Cancer Programme, Lisbon, Portugal.
*These authors contributed equally to this work.
[†]Corresponding authors. Email: ines.ramos@research.fchampalimaud.org (M.I.P.R.); L.Meyaard@umcutrecht.nl (L.M.)

Abstract

Leukocyte-associated immunoglobulin-like receptor-1 (LAIR-1) is an inhibitory receptor that is widely expressed in the immune system and recognizes collagens and collagen domain–containing proteins. The abundant presence of both LAIR-1 and its ligands implicates tight regulation of this interaction. Macrophage receptor with collagenous structure (MARCO) is a scavenger receptor that contains a collagen-like domain and is highly abundant on immunosuppressive macrophages. Here, we identified MARCO as a previously uncharacterized ligand for LAIR-1. We showed that MARCO interacted with LAIR-1 and induced inhibitory signaling by LAIR-1 in trans in human natural killer (NK) cells. MARCO and LAIR-1 were co-expressed by human macrophages in tumors and after stimulation with the cytokine interleukin-10 (IL-10) in vitro. Through single-molecule fluorescence microscopy, we demonstrated that MARCO and LAIR-1 also interacted in cis. The scavenger function of MARCO on human macrophages was unaffected by its in cis interaction with LAIR-1. In contrast, this interaction with MARCO reduced both the binding of collagen to LAIR-1 and its signaling response to collagen. Indeed, LAIR-1–mediated inhibitory function was increased after CRISPR/Cas9-mediated knockout of MARCO in IL-10–polarized primary human monocyte-derived macrophages. Our results identify a previously uncharacterized mechanism of LAIR-1 signaling regulation, whereby co-expression of MARCO suppresses the function of this inhibitory receptor. Thus, the induction of MARCO on immunosuppressive macrophages could lead to enhancement of their function through the release of LAIR-1–mediated inhibition.

Introduction

Leukocyte-associated immunoglobulin-like receptor-1 (LAIR-1) is an inhibitory immunoreceptor that is found on a wide range of immune cells[1–7]. Upon ligation, LAIR-1 suppresses immune cell function, T cell and natural killer (NK) cell cytotoxicity, and cytokine production by monocytes[8–10]. Collagens, collagen fragments, and proteins with collagenous domains, such as the complement component C1q, mannose-binding lectin (MBL), surfactant D (SP-D), and collectin-12, are ligands for LAIR-1[1–6]. The widespread expression of both LAIR-1 and its ligands prompts the question of how the activity of this inhibitory receptor is regulated to enable appropriate immune cell activation, but avoid pathologic immune activation[11]. We and others previously showed that the expression of LAIR-1 at the plasma membrane is regulated both at the level of gene transcription and by posttranscriptional shedding at the cell surface[10,12,13]. Furthermore, LAIR-2, a soluble homolog of LAIR-1[14], functions as a decoy receptor and competes for the same ligands[15,16]. Whether additional mechanisms that regulate LAIR-1 expression or accessibility exist is currently unknown.

We and others previously showed that blockade of the interaction between LAIR-1 and collagen promotes anti-tumor immunity in preclinical cancer models[17–20]. Specific immune cell subsets are differentially associated with tumor progression across various cancers[21,22]. The presence of macrophages, in particular immunosuppressive tumor-associated macrophages (TAMs), is primarily associated with shorter patient survival[21,23,24]. Multiple studies showed that macrophage receptor with collagenous structure (MARCO) is highly abundant on immunosuppressive TAMs[25–29]. MARCO is a scavenger receptor that is expressed primarily on macrophages, including Kupffer cells and alveolar macrophages[30–32], and plays a key role in the clearance of a wide array of potentially inflammatory ligands, including lipopolysaccharides and inorganic materials, such as asbestos[33,34]. As a member of the class A family of scavenger receptors[32], MARCO contains a collagenous domain. Because TAMs can also express LAIR-1[35], here, we investigated whether MARCO could act as a ligand for LAIR-1 and whether a possible interaction between MARCO and LAIR-1 in cis could have functional consequences.

Results

MARCO is a previously uncharacterized, functional ligand for LAIR-1

To determine whether MARCO was a potential ligand for LAIR-1, we tested the binding of a LAIR-1-Fc fusion protein to MARCO-overexpressing cells by immunofluorescence (Fig. 1A) and flow cytometry (Fig. 1B). We found that LAIR-1 bound to cell-expressed MARCO. This interaction was conserved between species, because mouse LAIR-1, human LAIR-1, and human LAIR-2 all bound to both mouse and human MARCO, although mouse LAIR-1 bound to a lesser extent (fig. S1A). We next confirmed the binding of MARCO to LAIR-1 by surface plasmon resonance (SPR) (Fig. 1C). We observed similar kinetics for the binding of LAIR-1 to collagen I and MARCO (Fig. 1C). The interactions between LAIR-1 and both collagen I and MARCO were non-monomeric, which did not allow for accurate KD determination using a 1:1 kinetic model. Binding affinities could be estimated to be in a double-digit nanomolar range.

Next, we used biolayer interferometry to determine the effect of MARCO binding to LAIR-1 on its further interaction with collagen I (Fig. 1D). We observed that in absence of MARCO, collagen I showed substantial binding to sensor-captured LAIR-1. However, when we presented MARCO to LAIR-1 first, it substantially reduced further collagen I binding (Fig. 1D). To exclude the possibility that LAIR-1 interacted with the scavenger receptor cysteine-rich (SRCR) domain, we transfected HEK293T cells with plasmids encoding MARCOII, a natural variant of MARCO lacking the SRCR domain[36], or full-length MARCO, and assessed LAIR-1-Fc fusion protein binding to these cells (Fig. 1, E and F). We found that LAIR-1 bound equally to MARCOII-expressing cells and to MARCO-expressing cells, suggesting that LAIR-1 binds to the collagenous domain of MARCO. This suggests that MARCO is capable of interfering with the binding of collagen to LAIR-1. LAIR-1 has a high-affinity collagen binding domain[37], which makes it likely that MARCO and collagens compete for the same binding site in LAIR-1, but we have no formal proof for this assumption.

Next, we determined whether the interaction between MARCO and LAIR-1 could induce LAIR-1 signaling. Collagen activates NFAT-GFP 2B4 reporter cells ectopically expressing chimeric LAIR-1-CD3ζ[1] (Fig. 1G). We found that plate-bound recombinant MARCO induced LAIR-1-CD3ζ–mediated GFP expression to a similar extent as that induced by other LAIR-1 ligands, such as collagen, supporting a role for MARCO as a functional LAIR-1 ligand (Fig. 1G, Table 1). Additionally, we found that MARCO inhibited Fc receptor–mediated activation of functional LAIR-1-expressing NF-κB-SEAP THP-1 reporter cells[38], and that this inhibition could be reversed by the addition of a blocking anti-LAIR-1 antibody (fig. S1B). Because the class A family of scavenger receptors all contain collagenous domains, we tested whether other class A family members also functioned as LAIR-1 ligands. We found that macrophage scavenger receptor 1 (MSR1, also known as SCARA1), SCARA3, and SCARA5 did not elicit reporter activity, whereas collectin-12 (SCARA4) stimulated reporter activation (fig. S1C, Table 1), consistent with previous findings[4].

We next studied whether cell-expressed MARCO induced inhibitory signaling in LAIR-1-expressing cells in trans. We performed a cytotoxicity assay with the YT.2C2 NK cell line ectopically expressing LAIR-1 as effector cells and the MHC-I–negative 721.221 EBV-B cell line as target cells[8]. Consistent with previous findings, WT YT.2C2 cells killed WT, Coll-XVII$^+$, and CD32$^+$ target cells to a similar extent (fig. S1D), whereas LAIR-1-expressing YT.2C2 cells had significantly reduced killing capacity when the target cells expressed the transmembrane collagen Coll-XVII or had anti–LAIR-1 antibody bound to CD32 (Fig. 1H). Similarly, LAIR-1-expressing YT.2C2 cells showed reduced killing of target cells expressing MARCO (Fig. 1H). Together, these data suggest that MARCO is a previously uncharacterized functional ligand for LAIR-1.

LAIR-1 and MARCO are co-expressed on macrophages and can interact in cis

We next assessed mRNA expression of *MARCO* and *LAIR1* in publicly available single-cell RNA-sequencing (scRNA-seq) data of myeloid cells from patients with melanoma, lung cancer, or breast cancer[39–45]. We found that 4 to 30% of tumor-infiltrating macrophages expressed only *MARCO* and not *LAIR1*, whereas 17 to 34% expressed both *LAIR1* and *MARCO* (Fig. 2A). Note that we found that most (54 to 82%) of the *MARCO*-expressing cells also expressed *LAIR1* (Fig. 2B), indicating that LAIR-1 and MARCO show a high degree of co-expression in the immune infiltrate of tumors. We differentiated human monocytes, which do not express MARCO under basal conditions, with M-CSF to monocyte-derived macrophages (MDMs) in vitro. Subsequent polarization with IL-10 resulted in significant co-expression of LAIR-1 and MARCO compared to unpolarized MDMs (Fig. 2, C and D).

We therefore studied whether co-expression of MARCO and LAIR-1 resulted in a cis interaction. Furthermore, because multiple isoforms of LAIR-1 have been described, including the canonical isoform LAIR-1a and LAIR-1b, an isoform that lacks 17 amino acid residues containing multiple O-linked glycosylation sites[46,47], we also determined whether the shortened stalk region of LAIR-1b affected this interaction. We expressed SNAP-tagged LAIR-1a or LAIR-1b with MARCO-HaloTag in THP-1$^{LAIR1-/-}$ cells to a single molecule–compatible level with inducible promoters and then used total internal reflection fluorescence (TIRF) microscopy to determine protein mobility at the single-molecule level (Fig. 3, A to C). We found that both LAIR-1a and LAIR-1b were more mobile than MARCO (Fig. 3D). MARCO co-expression reduced the mobility of LAIR-1a, but not LAIR-1b, in the membrane (Fig. 3E). We next added a blocking anti-LAIR-1 antibody, which inhibited the interaction between LAIR-1 and MARCO or collagen (fig. S2A). The addition of this antibody, but not of an isotype control, restored LAIR-1a mobility in the presence of MARCO, whereas LAIR-1b mobility was unaffected (Fig. 3E). These data indicate that LAIR-1a and MARCO interact in cis, immobilizing LAIR-1a in THP-1 cell membranes. Together, our data show that LAIR-1 and MARCO can be co-expressed on macrophages in vitro and that the two receptors can interact in cis.

The interaction between LAIR-1 and MARCO in cis blocks collagen binding to LAIR-1

Next, we determined whether the cis interaction between LAIR-1 and MARCO interfered with the function of either receptor. We first tested the effect of the co-expression of LAIR-1 and MARCO on MARCO function. We used *E. coli* BioParticles labelled with pHrodo to monitor phagocytosis mediated by MARCO on IL-10–polarized MDMs[48] by live-cell imaging, because the involvement of MARCO in *E. coli* binding and uptake was described previously in several studies[31,48,49]. We blocked the interaction between LAIR-1 and MARCO with the anti-LAIR-1 antibody, as shown earlier (fig. S2A), or with a LAIR-2-Fc fusion protein that is a LAIR-1 antagonist[14]. In both conditions, the phagocytic capacity of IL-10–polarized macrophages was unaffected (Fig. 4, A and B).

We then tested the effect of MARCO co-expression on LAIR-1 function. We overexpressed MARCO in LAIR-1-CD3ζ NFAT-GFP reporter cells and observed that, during extended culture periods in the absence of other ligands, there was no increased induction of GFP compared with LAIR-1-CD3ζ NFAT-GFP cells that did not express MARCO. This implies that in contrast to their interaction in trans, the interaction between MARCO and LAIR-1 in cis did not result in active signaling by LAIR-1 (fig. S2B). However, we observed that collagen-induced signaling in LAIR-1a-CD3ζ NFAT-GFP reporter cells, and to a lesser extent in LAIR-1b-expressing reporter cells, was decreased significantly in the presence of MARCO co-expression (Fig. 4C). This suggests that MARCO co-expression impairs collagen-induced LAIR-1 signaling by blocking the collagen-binding domain of LAIR-1. To test this, we assessed the binding of collagen IV-FITC to LAIR-1-expressing cells in the absence or presence of MARCO co-expression. We found for both LAIR-1a and LAIR-1b that LAIR-1$^+$MARCO$^+$ THP-1 cells bound less collagen IV-FITC (as measured by the reduced mean fluorescence) than did LAIR-1$^+$MARCO$^-$ cells (Fig. 4D).

Together, these data suggest that whereas MARCO function is unaffected by its cis interaction with LAIR-1, the co-expression of MARCO on LAIR-1$^+$ cells can interfere with LAIR-1–collagen binding and signaling, which could lead to the decreased inhibitory function of LAIR-1. To test this hypothesis in primary cells, we used CRISPR/Cas9 to knockout MARCO or LAIR-1 in primary human monocytes and generated IL-10-polarized MDMs lacking either MARCO or LAIR-1 (Fig. 5, A and B, fig. S3, A to D). The efficiency of target knockout (KO) differed per gene, such that the average MARCO KO efficiency was 61% (range: 51 to 71%) and the average LAIR-1 KO efficiency was 77% (range: 61 to 89%). We then assessed LPS-induced IL-8 secretion by the IL-10-polarized MDMs, which were seeded on plate-immobilized BSA or collagen I (Fig. 5C, fig. S3E). In control CRISPR MDMs, exposure to collagen resulted in a 15% inhibition of IL-8 secretion compared to exposure to BSA in cells from all donors (Fig. 5D). MARCO-deficient MDMs showed significantly increased inhibition of IL-8 secretion in cells from five of seven donors. In contrast, LAIR-1–deficient MDMs showed significant potentiation of IL-8 secretion in cells from all donors. Thus, the inhibition of IL-8 secretion by collagen I is mediated by LAIR-1 and, in cells from five of seven donors, co-expression of MARCO impaired this inhibitory function of LAIR-1. Note that the two donors for

which knockdown of LAIR-1 had the greatest effect on LAIR-1–mediated inhibition of IL-8 were the same donors for which removal of MARCO did not further improve LAIR-1 function. Hence, we conclude that MARCO limits the capacity of LAIR-1 to inhibit immune responses by primary human macrophages (Fig. 5E).

Low MARCO and LAIR-1 expression is associated with increased survival in GBM and LUSC

To determine the clinical context in which this interaction between LAIR-1 and MARCO might play a role, we assessed the expression of *LAIR1* and *MARCO* mRNAs in publicly available data from the cancer genome atlas (TCGA)[50]. Consistent with the high degree of co-expression of *MARCO* and *LAIR1*, we found that *LAIR1* expression was significantly increased in tumor samples with high (top quartile) *MARCO* expression from patients with glioblastoma multiforme (GBM) and lung squamous cell carcinoma (LUSC), compared to samples with low (bottom quartile) *MARCO* expression (Fig. 6A). We then stratified patients with GBM and LUSC based on their expression of *MARCO* and *LAIR1* in tumors and found that low expression of either *MARCO* or *LAIR1* in tumors was associated with increased median overall survival compared to that for samples with high expression (Fig. 6B). Moreover, low expression of both *MARCO* and *LAIR1* was associated with a further increase in median overall survival (Fig. 6C). Our findings suggest that macrophages co-expressing MARCO and LAIR-1 are associated with disease progression in GBM and LUSC.

Discussion

Here, we showed that the scavenger receptor MARCO is a previously uncharacterized functional ligand for LAIR-1. We found that MARCO and LAIR-1 were co-expressed on macrophage subsets in tumors and could interact in vitro in cis. MARCO antagonized collagen-induced LAIR-1 signaling in cis by acting as a decoy receptor, whereas LAIR-1 had no effect on the scavenger receptor function of MARCO. LAIR-1 is an inhibitory pattern recognition receptor that interacts with various types of collagen and collagen-like domains[1–3,51]. This array of LAIR-1–binding proteins also includes transmembrane receptors, including collectin-12, layilin, and chondrolectin[4]. These proteins are primarily expressed on non-hematopoietic cells, such as epithelial cells and neurons[52–54], where they likely function as immunosuppressive ligands for LAIR-1 in trans. Similarly, we demonstrated that MARCO induced LAIR-1 signaling in trans. Unlike previously described LAIR-1 ligands, MARCO can be simultaneously expressed with LAIR-1 on the same cell, and such co-expression resulted in antagonism of LAIR-1 in cis.

A number of inhibitory receptors can interact with their ligands in cis, including PD-L1, CD22, and LILRB1[55–57]. These interactions block inhibitory signaling by trans ligands, or conversely result in constitutive inhibitory signaling that increases the threshold for activation[56,57]. Our finding that LAIR-1 signaling is induced by binding to MARCO in trans, but not in cis, raises the question of how interactions between LAIR-1 and its ligands result in downstream signaling. It is possible that the binding interface on MARCO that is accessible to LAIR-1 is more limited when MARCO interacts in cis due to the reduced accessibility in the z-dimension, because both molecules are tethered to the same cellular membrane, and due to constant lateral membrane diffusion of LAIR-1:MARCO complexes. Additionally, the interaction between MARCO and LAIR-1 in trans, but not in cis, could result in the accumulation of LAIR-1 in close contacts between the two opposing cell membranes, enabling the kinetic-segregation (KS) model of immune receptor activation[58].

MARCO expression is often induced during the differentiation of human macrophages toward M2-like phenotypes[59], including tumor-associated macrophages, whereby it is able to interact with LAIR-1 on the cell membrane in cis. We showed that the cis interaction between LAIR-1 and MARCO inhibited collagen-induced LAIR-1 signaling, suggesting that this interaction could suppress LAIR-1 function by preventing collagen binding during M2-like macrophage polarization. Conversely, the binding of LAIR-1 to MARCO did not affect the scavenging role of MARCO, suggesting that its interaction with LAIR-1 does not change MARCO signaling. Because MARCO has both a collagen domain, to which LAIR-1 binds, and a SRCR domain, such differences in the cross-regulation of LAIR-1 and MARCO are likely due to separate domains on MARCO interacting with LAIR-1, material for engulfment[36], or both.

Note that upon CRISPR/Cas9-mediated KO of LAIR-1 in IL-10–polarized MDMs, we observed potentiation of IL-8 secretion by collagen I as compared to BSA, in contrast to the inhibition of IL-8 secretion by control CRISPR MDMs. It is possible that in the absence of LAIR-1, the presence

of activating collagen receptors on the IL-10–polarized MDMs induced this potentiation, because the activation of osteoclast-associated receptor (OSCAR) on monocytes by collagen I can induce IL-8 secretion[60]. However, we did not assess the expression of activating collagen receptors in our system.

In contrast to LAIR-1b, LAIR-1a has multiple glycosylation sites in its stalk region[47]. By tracking the motion of single LAIR-1 and MARCO molecules in the plasma membrane by TIRF imaging, we found that co-expression of MARCO decreased the mobility of LAIR-1a but not that of LAIR-1b, consistent with the very minor effect of MARCO on collagen-induced LAIR-1b signaling. However, co-expression of MARCO inhibited the binding of collagen to both LAIR-1a and LAIR-1b. Thus, co-expression of MARCO and LAIR-1b did not affect the mobility of LAIR-1b, but did interfere with its ability to bind to collagen. The reason for this is unclear. It is possible that the glycosylation of LAIR-1a contributes to a more stable interaction with MARCO or that the shorter stalk region of LAIR-1b affects its flexibility and thus its ability to bind to MARCO.

Regulation of the expression of inhibitory receptors and their ligands is paramount for their role in orchestrating an appropriate immune response[11]. The expression of MARCO as a trans ligand could enable LAIR-1 on infiltrating immune cells to establish a threshold for activation. In contrast, the increased abundance of MARCO on LAIR-1–expressing immunosuppressive macrophages during activation and the high affinity of MARCO for LAIR-1 could interfere with the engagement of LAIR-1 with extrinsic factors presented in trans through its competition in cis, thus preventing the recognition of inhibitory cues from the microenvironment. In this way, MARCO not only supports increased pathogen or debris clearance, but also may prevent LAIR-1–mediated inhibition by other ligands such as collagen and C1q that have similar affinities for LAIR-1[3]. The same mechanisms might exacerbate disease in the context of tumor development. Release of the inhibition of myeloid cells through LAIR-1:collagen signaling as a result of a cis interaction between LAIR-1 and MARCO could promote macrophage-mediated tumor progression. Consistent with this, myeloid-specific knockout of LAIR-1 in a metastatic melanoma model in mice results in worse disease progression[4]. Furthermore, it would be interesting to determine to what extent the interaction between MARCO and LAIR-1 contributes to the association of MARCO expression with tumor progression in multiple cancers. Considering that some studies have explored the potential for MARCO as a target in cancer immunotherapy[25,26,61], our findings introduce a previously uncharacterized aspect to LAIR-1 and MARCO biology in the context of cancer. Because the low expression of both *MARCO* and *LAIR1* appears to correlate with prolonged patient survival, it would be interesting to determine how these receptors also interact in vivo and whether this could be utilized to inform therapeutic targeting of either receptor or assist in patient selection for effective therapy. Together, the identification of MARCO as a previously uncharacterized ligand for LAIR-1 that can interact in cis reveals a mechanism of LAIR-1 regulation that has possible therapeutic implications.

Materials and Methods

Cell lines

HEK293T cells were cultured in DMEM (Gibco #31966-021) supplemented with 10% fetal bovine serum (FBS, Sigma-Aldrich #F7524) and 1% penicillin/streptomycin (P/S) (Gibco #P0781) at 37°C and 5% CO_2. Parental and transduced 2B4-NFAT-GFP reporter cells[1] and THP-1 NF-κB reporter cells were cultured in RPMI 1640 (Gibco #52400-025) with 10% FBS and 1% P/S. Parental and transduced YT.2C2, THP-$1^{LAIR1-/-}$, and LCL 721.221 cells were cultured in RPMI 1640 with 10% FCS, 1% P/S, and 2 mM L-glutamine (Gibco #25030024). Cell lines were routinely screened for mycoplasma and tested negative.

Transfections

HEK293T cells (1.3 x 10^6 cells) were seeded in T25 flasks 24 hours before transfection. PEI:DNA complexes were formed by mixing 15 µg of PEI MAX (Polysciences #24765) and pcDNA3.1 hygro vectors encoding MARCO or MARCOII in a 3:1 PEI:DNA ratio in plain DMEM, and were incubated for 20 min at room temperature. The vectors were kindly provided by the Bowdish lab[36]. HEK293T cells were transfected by incubation with the PEI:DNA mixture for 8 hours in a 5% CO_2 humidified 37°C incubator. Cells were left for approximately 48 hours before undergoing LAIR-1-Fc staining.

Lentivirus production and transduction

HEK293T cells were seeded in a 6-well plate at a density of 0.5 to 0.6 x 10^6 cells per well and allowed to settle overnight at 37°C, 5% CO_2. The cells were then transfected with lentiviral plasmids using the Fugene HD transfection reagent (Promega #E2311). Virus-containing cultured medium was used to transduce target cells (2B4 reporter lines and THP-$1^{LAIR1-/-}$ cells) as described previously[1,62]. Expression was assessed by flow cytometry on a FACSFortessa flow cytometer (BD), and transduced cells were sorted with a FACSAriaIII (BD).

Glass coverslip and imaging chamber preparation for TIRF imaging

We treated 22x22 mm glass coverslips (#1.5 Menzel Gläser; VWR #631-0851) with a total of 8 drops of Piranha solution [3:1 concentrated H_2SO_4 (Sigma-Aldrich #258105):30% H_2O_2 (Sigma-Aldrich #216763)] for at least 1 hour to remove impurities from the glass surface and enable uniform coating with poly-L-lysine (PLL; Sigma-Aldrich #P8920). Eppendorf tubes (0.5-ml) were cut at the inflection point between the conical and cylindrical part of the tube, and their lids were removed. The lip of the remaining cylindrical part of the tube was then coated with UV-curing glue (Norland Optical Adhesive 68, Norland Products Inc.) and stored in an Eppendorf tube rack with the UV-curing glue pointing upwards while the glass coverslips were incubating with Piranha solution. The glass slides were then rinsed thoroughly with Milli-Q water and blow-dried using a stream of compressed nitrogen gas to prevent water evaporation and residue deposition on the clean coverslips. Once dried, the coverslips were placed with their clean side facing the glue-covered lip of the Eppendorf tube. Once a continuous ring of glue had formed between the glass coverslip and the Eppendorf tube lip, the tube rack holding the uncured imaging chambers was

placed beneath a UV lamp for 3 min to cure the UV-sensitive glue. The assembled chambers were then gently removed from the rack, placed on a glass dish, and transferred to a plasma cleaner. The pressure in the vacuum chamber of the plasma cleaner was then reduced to 0.3 Torr before activating the plasma discharger. The slides were plasma-treated for 13 min to render them hydrophilic and enable efficient adsorbance of PLL onto the glass surface. Concurrent with the plasma treatment of the glass slides, 100 µl of a 0.5 mg/ml solution of PLL in Milli-Q was prepared for each imaging chamber (two-fold dilution from a 0.1% stock solution). Then, 100 µl of the 0.5 mg/ml PLL solution in Milli-Q was added to each imaging chamber immediately upon removal of the imaging chambers from the plasma cleaner. The slides were incubated with PLL solution for at least 1 hour, taking care not to let the coverslips dry out, and were only washed with 5 x 200 µl of HEPES-buffered saline [40 mM HEPES, 140 mM NaCl, (pH 7.6)] immediately before cells were deposited onto the coverslips.

Cell labeling for TIRF imaging

For TIRF microscopy, LAIR-1a-SNAP-tag–, LAIR-1b-SNAP-tag–, LAIR-1a-SNAP-tag/MARCO-HaloTag–, and LAIR-1b-SNAP-tag/MARCO-HaloTag–expressing THP-$1^{LAIR1-/-}$ cells were stimulated with 0.1 µg/ml tetracycline (Sigma-Aldrich #T3258) to induce protein expression 24 hours before imaging. On the day of imaging, 40 µl of cell suspension was mixed with 40 µl of 0.4% trypan blue solution (Gibco #15-250-061) and counted with the Luna II cell counter (Logos Biosystems). Cell culture volumes corresponding to 1 million cells were collected from the cell culture flasks into 5-ml Eppendorf tubes and centrifuged at 125*g* in a tabletop centrifuge for 5 min. The supernatant was then replaced by 1 ml of pre-warmed staining solution [RPMI 1640 phenol red free (VWR #392-0430), 10% FBS, 1% GlutaMAX (Gibco #35050038), 1% HEPES buffer (Lonza BioWhittaker #17-737E)], and containing either 100 nM each of Janelia Fluor X 650 Halo-tag ligand and Janelia Fluor X 554 cpSNAP-tag ligand when staining MARCO-Halo-tag– and LAIR-1-SNAP-tag–expressing cells or 100 nM Janelia Fluor X 554 cpSNAP-tag ligand when staining cells expressing LAIR-1-SNAP-tag only. Cells resuspended in staining solution were transferred to a 24-well plate and incubated at 37°C, 5% CO_2 for 1 hour. After staining, cell suspensions were transferred to 5-ml Eppendorf tubes and centrifuged at 125*g* in a tabletop centrifuge for 5 min. The supernatant was removed and replaced by 1 ml of pre-warmed washing/imaging buffer (RPMI 1640 phenol red free, 10% FBS, 1% GlutaMAX, 1% HEPES). Cells resuspended in the washing buffer were transferred to a 24-well plate and incubated at 37°C, 5% CO_2 for 10 min. This washing step was repeated twice more, after which the 1 ml of cell suspension was either transferred to a 24-well plate and divided into several aliquots for incubation with antibodies or transferred directly to the PLL-coated glass slides for TIRF imaging. For blocking experiments, cells were stained with fluorescently labeled SNAP-tag or HaloTag ligands, as described earlier, and incubated with blocking (anti-LAIR-1, produced in-house) or isotype control (anti–keyhole limpet hemocyanin, produced in-house) antibodies at a concentration of 50 µg/ml for 30 min at 37°C, 5% CO_2 by directly adding the antibody solution to the cell suspension in the 24-well plates. To keep the incubation time of each sample with antibodies the same, the stained cell “stock” was divided into aliquots of 250 µl

(corresponding to 250,000 cells) before staggered antibody addition. After incubating the cells for 30 min with antibodies in the 24-well plate at 37°C, 5% CO_2, cells were deposited onto PLL-coated imaging chambers and incubated for 30 min at 37°C, 5% CO_2.

TIRF imaging

The samples were imaged with a K2 custom-built total internal reflection fluorescence microscope[63]. Each sample was imaged for 30 min while maintaining the sample temperature at 37°C through coupling with a heated 100x oil objective. After finding cells displaying suitable MARCO-HaloTag expression (10 to 25% of all cells in each sample), the samples were bleached in a circular area approximately 25 µm in diameter by exposing them for 3 s continuously to a 561-nm laser at 100% laser power. This resulted in an almost complete loss of signal stemming from the LAIR-1-SNAP-tag labeled with Janelia Fluor cp554-SNAP-tag ligand in the bleached area, which was gradually repopulated by diffusion of fluorescently labeled LAIR-1 from unbleached areas of the cell, consequently yielding signal levels adequate for single-molecule tracking. The samples were then imaged for either 1000 frames (100 s at 100-ms exposure time) in the case of $MARCO^+LAIR\text{-}1^+$ THP-1 cells, or for 500 frames (50 s at 100-ms exposure time) in the case of LAIR-1-only expressing cells. The signals from each of the three channels were acquired simultaneously.

Single-particle tracking

The data acquired as described earlier were subjected to single-particle tracking analysis with Single Particle Interaction Tracking (SPIT) software developed in-house[64]. SPIT uses a minimum net gradient to localize particles in each frame of each individual channel separately (for the data presented here, the gradient was 400 for both channels). The algorithm then links localizations frame by frame into tracks for each individual channel, while considering a specified window of tolerance both in the spatial distance (for the data presented here, the search radius was 4 pixels, or 4 x 108 nm = 432 nm) and in the temporal separation from the previous localization (for the data presented here, 4 frames, corresponding to 400 ms). From the tracks, we extracted jump distances between localizations within the same track, which were used to assess the difference in mobility between MARCO and LAIR-1, as well as between the different LAIR-1 isoforms.

FITC labeling of collagen IV

Fluorescein isothiocyanate (FITC; Fisher Scientific #F1906) was dissolved in DMSO (Sigma-Aldrich #D5879) at a concentration of 10 mg/ml. FITC-DMSO was added to 1 ml of 1 mg/ml human collagen IV (Sigma-Aldrich #C5533-5MG) at a 48:1 molar ratio and dialyzed on a rotor against 1x FITC labeling buffer [0.5 M Boric acid, 2 M NaCl, (pH 9.2)] for 3 hours at 4°C. Labeled collagen IV was then dialyzed against PBS overnight at 4°C, which was followed by a final dialysis against PBS for 3 hours.

Monocyte isolation and CRISPR/Cas9–mediated gene editing

In accordance with the declaration of Helsinki and approved by the University Medical Centre Utrecht (UMCU) medical ethical committee (07–125/O), blood from healthy donors (three males and ten females, age range 24 to 64 years) was collected in lithium-heparin tubes (BD) after informed consent. Peripheral blood mononuclear cells (PBMCs) were isolated from healthy donor blood by Ficoll-Paque gradient (Cytiva #17144003). Fresh monocytes were isolated with human anti-CD14 microbeads (Miltenyi Biotec #130-050-201) by manual magnet-assisted cell sorting (MACS) using LS columns (Miltenyi Biotec #130-042-401), according to the manufacturer's instructions. MARCO and LAIR-1 were knocked out in monocytes using CRISPR/Cas9 as follows. Alt-R negative control crRNA #2 (IDT #1072545), MARCO crRNA (IDT; TACCTGATCCTGCTCACCGC), or LAIR-1 crRNA (IDT; CCCGGCACACGAAAGTCACA) was mixed with Alt-R tracrRNA (IDT #1072533) at equimolar concentrations and heated at 95°C for 5 min to form gRNAs. Alt-R S.p. Cas9 Nuclease 3NLS (IDT #1074182) was added at a molar ratio Cas9:gRNA of 1:1.83 and incubated for 20 min at room temperature to form Cas9-gRNA RNPs. 4 µM Alt-R Cas9 electroporation enhancer (IDT #1075916) was added and incubated for 5 min at room temperature, before adding the RNPs to the Nucleovette strip of the P3 Primary Cell 4D-Nucleofector X Kit S (Lonza #V4XP-3032). Monocytes were centrifuged at 100*g* for 10 min at room temperature, 1 x 10^6 cells were resuspended in 20 µl of P3 solution, added to the Nucleovette strip, and nucleofection was performed with the Lonza 4D Nucleofector (Lonza) using the CM-137 program. Immediately after nucleofection, 180 µl of prewarmed macrophage differentiation medium [RPMI 1640 supplemented with 10% FCS, 1% p/s, 2 mM L-glutamine, 10 mM HEPES (Gibco #15630-056), and 50 ng/ml M-CSF (PeproTech #300-25; equivalent to ≥50 IU/ml)] was added to each well, left in a 5% CO_2 humidified 37°C incubator for 10 min to recover, and then cells were harvested by gently pipetting. CRISPRed monocytes (5 x 10^5 cells per well) were added to tissue culture–treated 12-well plates (Corning).

Macrophage differentiation

Macrophages were generated by plating isolated monocytes at a density of 3 x 10^5 cells/ml in macrophage differentiation medium for 6 days, and additional M-CSF (50 ng/ml) was added on day 3. For IL-10 polarization, 20 ng/ml recombinant human IL-10 (PeproTech #200-10; equivalent to ≥10 IU/ml) was added for another 24 hours.

Functional assay of collagen-induced LAIR-1 signaling

BSA (5 µg/ml; Roche # 10735094001) or human collagen I (5 µg/ml; Sigma-Aldrich #C7774) was coated onto 96-well F-bottom plates (Thermo Scientific) for 3 hours at 37°C and 5% CO_2. Macrophages were harvested with Accutase (Sigma-Aldrich #A6964), centrifuged for 10 min at 500*g*, and resuspended in macrophage differentiation medium without M-CSF. Macrophages (20,000 to 40,000; where the number of macrophages was kept equal per donor) were added to each well, centrifuged for 3 min at 54*g* and pre-incubated for 2.5 hours in a 5% CO_2 humidified

37°C incubator. Subsequently, the macrophages were treated with 100 ng/ml ultrapure LPS from *E. coli* (Invivogen #tlrl-3pelps) for 20 hours, and cell-free supernatant was harvested and stored at -20 °C.

ELISA for IL-8

Secreted IL-8 in the cell-free supernatant was quantified with a commercial IL-8 ELISA kit (Invitrogen #88-8086-88) and MaxiSorp 96-well plates (Thermo Scientific) according to the manufacturer's protocol with overnight sample incubation at 4°C. Optical density (OD) values at 450 and 570 nm were measured with the CLARIOstar plate reader (BMG Labtech). OD values at 570 nm were subtracted from those at 450 nm, and these corrected values were used for ELISA analysis using a four-parameter dose-response curve for the standard curve with GraphPad Prism. Due to baseline differences in IL-8 secretion, IL-8 secretion was normalized to the BSA-coated samples per donor per CRISPR condition, or inhibition was calculated using the following formula per donor per CRISPR condition:

$$\frac{IL{-}8\ secretion\ BSA\ well - IL{-}8\ secretion\ collagen\ I\ well}{IL{-}8\ secretion\ BSA\ well} \times 100\%.$$

Flow cytometry

For flow cytometry analysis of macrophages, cells were harvested with Accutase and single-cell suspensions were made. Cells were then washed with PBS and stained with Fixable Viability Dye eFluor 780 (eBioscience #65-0865-14) for 20 min at room temperature in the dark. The cells were then washed with FACS buffer (PBS, 0.1% BSA, 0.01% NaN_3) and blocked with 5% normal mouse serum (NMS; Fitzgerald #88-NM35-50ML) for 15 min at room temperature. Subsequently, antibody mixes containing 5% NMS were added, and surface markers were stained for 30 min at 4°C with αLAIR-1-BV421 (BD #744557 RRID:AB_2742321) and αMARCO-AF647 (produced in-house). Cells were then washed twice with FACS buffer, resuspended in FACS buffer, and acquired on a FACSFortessa flow cytometer (BD). For two-step staining for LAIR-1-Fc fusion protein binding (produced in-house), cells were detached with 2 mM EDTA in PBS for 15 min at 37°C and 5% CO_2, stained with Fixable Viability Dye eFluor 780 for 20 min at room temperature in the dark, washed once with FACS buffer, incubated with 10 µg/ml (un)biotinylated LAIR-1-Fc at 4°C, washed twice with FACS buffer after primary staining, and then stained with secondary antibodies (anti-IgG1-PE or Streptavidin-PE BD #349023) for 30 min at 4°C, followed by two washes with FACS buffer, before acquisition on a FACSFortessa (BD). For collagen IV-FITC staining, parental and MARCO-transduced LAIR-1–expressing THP-1 cells were incubated with collagen IV-FITC and unconjugated anti-LAIR-1 (clone DX26; produced in-house) for 30 min on ice. The cells were then washed with FACS buffer, which was followed by staining with anti-IgG-AF647 (Invitrogen #A21235 RRID:AB_2535804) for 25 min on ice. Cells were washed with FACS buffer, resuspended in FACS buffer, and acquired on a FACSCanto flow cytometer (BD).

Reporter assay

Control antibodies [αCD3 (BD #553057 RRID:AB_394590) and αLAIR-1 (produced in-house)] or recombinant proteins [human collagen I, rat collagen I (Corning #354249), and human MARCO (R&D #7586-MA-050)] were immobilized on MaxiSorp (Invitrogen) plates for 24 hours at 4°C at a concentration of 5 μg/ml, or as indicated in the figure legends, in PBS. Plates were washed multiple times with PBS, before 50,000 to 100,000 reporter cells were added and cultured overnight at 37°C in the presence or absence of soluble antagonist antibodies (produced in-house). After incubation, the cells were harvested and washed with FACS buffer before being resuspended in FACS buffer and acquired on a LSRFortessa (BD) or FACSCanto (BD). For THP-1 reporter assays, isotype antibodies with a WT Fc tail were immobilized on MaxiSorp plates in the presence or absence of recombinant MARCO, after which THP-1 NF-κB-SEAP IRF-Luc reporter cells (InvivoGen) were incubated overnight at 37°C, 5% CO_2. SEAP secretion was then detected with QUANTI-Blue (InvivoGen).

Receptor screening

HEK293T cells were seeded at a density of 350,000 cells/ml in 384-wells and transfected with control expression vectors or an expression vector encoding MARCO with Lipofectamine 2000. After two days, the cells were incubated with a recombinant LAIR-1-IgG fusion protein, which was followed by staining with an anti-hIgG-AF647 antibody. The cells were then washed, fixed, and imaged.

Surface plasmon resonance study of LAIR-1 binding to MARCO and type I collagen

Surface plasmon resonance (SPR) studies were performed to investigate the interaction between LAIR-1, MARCO, and type I collagen with a Biacore T200 instrument (Cytiva). hLAIR-1-hFc (2 μg/ml) was captured by its Fc region on flow cells 2 and 3 of a series S Protein A sensor chip (Cytiva). A negative control Fc-fusion protein was captured on flow cell 4, whereas flow cell 1 was used as reference. The binding of human or mouse MARCO and type I collagen (Millipore #CC050) to surface-captured LAIR-1-Fc was investigated by injecting different concentrations of these proteins ranging from 6.25 to 200 nM at a flow rate of 30 μl/min. 1x PBS (pH 7.4) supplemented with 0.1% Tween was used as running buffer, and real-time kinetics were measured at 37 °C. Processed sensorgrams, where appropriate, were fit to a 1:1 Langmuir binding model using Biacore's kinetics evaluation software to determine the kinetic rate constants and affinities.

Simultaneous binding assessment of MARCO and collagen to LAIR-1 by biolayer interferometry

To demonstrate the effect of MARCO on the binding of LAIR-1 to collagen, we used a simple real-time, label-free biosensing platform based on biolayer interferometry (Octet, HTX) which is a "dip and read" system and can study several binding interactions in parallel. Three different anti-hFc capture Octet sensor tips (Sartorious) were first soaked in 1x PBS, pH 7.4, supplemented with 0.1% Tween and 0.1% BSA, for about 15 min before the experiment. All reagents were then transferred to a 384-well Octet plate for real-time binding measurements. The sensors were

stepwise immersed in wells containing (i) human LAIR-1-hFc (10 μg/ml) or an Fc fusion protein (negative control) for 10 min, (ii) purified polyclonal human IgG (30 μg/ml) to block any unoccupied sites, (iii) 200 nM human MARCO or buffer until the signal reached saturation, and (iv) 100 nM type I collagen. The binding signals were monitored in real-time using the Octet's acquisition software. Thirty-second buffer wash steps were added after each binding step.

Bioinformatics

Single-cell RNA-seq data from publicly available datasets was retrieved[39–45], and Scope[65] was used to determine the expression of *LAIR1* and *MARCO* among macrophage or myeloid clusters identified in the corresponding publications.

TCGA analysis

GBM and LUSC primary and recurrent tumor gene expression data were analyzed with Omicsoft Land B37 (Qiagen). Briefly, *LAIR1* expression (FPKM+0.1) was assessed in the top and bottom *MARCO* quartiles. Overall survival was plotted for tumors in either the top or bottom quartiles for *LAIR1* or *MARCO*.

Cytotoxicity assay

Parental and transduced YT.2C2 and LCL 721.221 cells were harvested and counted. LCL target cells were then washed with PBS, stained with 1 μM CellTrace Violet (Invitrogen #C34557) in PBS at a density of 30 × 10^6 cells/ml for 7 min at 37 °C, before quenching with 100% FCS, followed by subsequent washes with RPMI 1640 and 10% FCS. $CD32^+$ LCL cells were additionally incubated with 20 μg/ml anti-LAIR-1 (clone DX26, made in-house) for 30 min. LCL target cells (50,000) were then cultured together with the appropriate ratios of WT or LAIR-1^+ YT cells in U-bottom 96-wells plates (Thermo Scientific) for 4 hours at 37°C. After co-culture, the cells were harvested, washed with PBS, and stained with Fixable Viability Dye eFluor 780, according to the manufacturer's instructions. After staining, the cells were washed with FACS buffer, before being resuspended in FACS buffer and acquired on a FACSCanto flow cytometer (BD).

Phagocytosis assay

Unpolarized and IL-10–polarized macrophages were harvested with Accutase and allowed to reattach at a density of 0.125 to 0.15 × 10^6 cells/ml in black/clear flat-bottom 96-wells plates (Corning) overnight at 37°C. The medium was then aspirated, and the cells were incubated for 1 hour with the appropriate anti-LAIR-1 reagents, LAIR-2-Fc fusion protein, or isotype controls (all produced in-house; all at 20 μg/ml in 100 μl of medium) at 37°C. Then, 100 μl of a 50 μg/ml solution of pHrodo Green *E. coli* BioParticles (Invitrogen #P35366) was added, and the cells underwent live imaging at 20x magnification on an Incucyte imaging machine (Sartorius). Green fluorescence was quantified after top-hat segmentation (radius: 100 μm, threshold: 2 GCU), edge split (sensitivity: -20), and cleanup (hole fill: 50 μm^2, adjust size: 5 pixels), and additionally filtered on a minimum object size of 100 μm^2.

Statistical analysis

Data were graphed and analyzed in FlowJo (v10.6.2), GraphPad Prism (v10), or R (v4.2.2). Significance was determined as indicated in the figure legends, and significant differences are indicated in each graph: *$P \leq 0.05$; **$P \leq 0.01$; ***$P \leq 0.001$; ****$P \leq 0.0001$.

Supplementary Materials

Figs. S1 to S3.

References and Notes

1. Lebbink, R. J., de Ruiter, T., Adelmeijer, J., Brenkman, A. B., van Helvoort, J. M., Koch, M., Farndale, R. W., Lisman, T., Sonnenberg, A., Lenting, P. J. & Meyaard, L. Collagens are functional, high affinity ligands for the inhibitory immune receptor LAIR-1. *J. Exp. Med.* **203,** 1419–1425 (2006).
2. Vijver, S. V., Singh, A., Mommers-Elshof, E. T. A. M., Meeldijk, J., Copeland, R., Boon, L., Langermann, S., Flies, D., Meyaard, L. & Ramos, M. I. P. Collagen Fragments Produced in Cancer Mediate T Cell Suppression Through Leukocyte-Associated Immunoglobulin-Like Receptor 1. *Front. Immunol.* **12,** 733561 (2021).
3. Son, M., Santiago-Schwarz, F., Al-Abed, Y. & Diamond, B. C1q limits dendritic cell differentiation and activation by engaging LAIR-1. *Proc. Natl. Acad. Sci.* **109,** (2012).
4. Keerthivasan, S., Şenbabaoğlu, Y., Martinez-Martin, N., Husain, B., Verschueren, E., Wong, A., Yang, Y. A., Sun, Y., Pham, V., Hinkle, T., Oei, Y., Madireddi, S., Corpuz, R., Tam, L., Carlisle, S., Roose-Girma, M., Modrusan, Z., Ye, Z., Koerber, J. T. & Turley, S. J. Homeostatic functions of monocytes and interstitial lung macrophages are regulated via collagen domain-binding receptor LAIR1. *Immunity* **54,** 1511-1526.e8 (2021).
5. Olde Nordkamp, M. J. M., Boross, P., Yildiz, C., Jansen, J. H. M., Leusen, J. H. W., Wouters, D., Urbanus, R. T., Hack, C. E. & Meyaard, L. Inhibition of the Classical and Lectin Pathway of the Complement System by Recombinant LAIR-2. *J. Innate Immun.* **6,** 284–292 (2014).
6. Olde Nordkamp, M. J. M., van Eijk, M., Urbanus, R. T., Bont, L., Haagsman, H. P. & Meyaard, L. Leukocyte-associated Ig-like receptor-1 is a novel inhibitory receptor for surfactant protein D. *J. Leukoc. Biol.* **96,** 105–111 (2014).
7. Van Laethem, F., Donaty, L., Tchernonog, E., Lacheretz-Szablewski, V., Russello, J., Buthiau, D., Almeras, M., Moreaux, J. & Bret, C. LAIR1, an ITIM-Containing Receptor Involved in Immune Disorders and in Hematological Neoplasms. *Int. J. Mol. Sci.* **23,** 16136 (2022).
8. Meyaard, L., Adema, G. J., Chang, C., Woollatt, E., Sutherland, G. R., Lanier, L. L. & Phillips, J. H. LAIR-1, a novel inhibitory receptor expressed on human mononuclear leukocytes. *Immunity* **7,** 283–290 (1997).
9. Son, M. & Diamond, B. C1q-Mediated Repression of Human Monocytes Is Regulated by Leukocyte-Associated Ig-Like Receptor 1 (LAIR-1). *Mol. Med.* **20,** 559–568 (2014).

10. Carvalheiro, T., Garcia, S., Pascoal Ramos, M. I., Giovannone, B., Radstake, T. R. D. J., Marut, W. & Meyaard, L. Leukocyte Associated Immunoglobulin Like Receptor 1 Regulation and Function on Monocytes and Dendritic Cells During Inflammation. *Front. Immunol.* **11,** 1793 (2020).
11. Rumpret, M., Drylewicz, J., Ackermans, L. J. E., Borghans, J. A. M., Medzhitov, R. & Meyaard, L. Functional categories of immune inhibitory receptors. *Nat. Rev. Immunol.* **20,** 771–780 (2020).
12. Verbrugge, A., de Ruiter, T., Geest, C., Coffer, P. J. & Meyaard, L. Differential expression of leukocyte-associated Ig-like receptor-1 during neutrophil differentiation and activation. *J. Leukoc. Biol.* **79,** 828–836 (2006).
13. Ouyang, W., Xue, J., Liu, J., Jia, W., Li, Z., Xie, X., Liu, X., Jian, J., Li, Q., Zhu, Y., Yang, A. & Jin, B. Establishment of an ELISA system for determining soluble LAIR-1 levels in sera of patients with HFRS and kidney transplant. *J. Immunol. Methods* **292,** 109–117 (2004).
14. Lebbink, R. J., van den Berg, M. C. W., de Ruiter, T., Raynal, N., van Roon, J. A. G., Lenting, P. J., Jin, B. & Meyaard, L. The Soluble Leukocyte-Associated Ig-Like Receptor (LAIR)-2 Antagonizes the Collagen/LAIR-1 Inhibitory Immune Interaction. *J. Immunol.* **180,** 1662–1669 (2008).
15. Nordkamp, M. J. M. O., van Roon, J. A. G., Douwes, M., de Ruiter, T., Urbanus, R. T. & Meyaard, L. Enhanced secretion of leukocyte-associated immunoglobulin-like receptor 2 (LAIR-2) and soluble LAIR-1 in rheumatoid arthritis: LAIR-2 is a more efficient antagonist of the LAIR-1-collagen inhibitory interaction than is soluble LAIR-1. *Arthritis Rheum.* **63,** 3749–3757 (2011).
16. Lenting, P. J., Westerlaken, G. H. A., Denis, C. V., Akkerman, J. W. & Meyaard, L. Efficient Inhibition of Collagen-Induced Platelet Activation and Adhesion by LAIR-2, a Soluble Ig-Like Receptor Family Member. *PLoS ONE* **5,** e12174 (2010).
17. Xu, L., Wang, S., Li, J., Li, J. & Li, B. Cancer immunotherapy based on blocking immune suppression mediated by an immune modulator LAIR-1. *OncoImmunology* **9,** 1740477 (2020).
18. Ramos, M. I. P., Tian, L., de Ruiter, E. J., Song, C., Paucarmayta, A., Singh, A., Elshof, E., Vijver, S. V., Shaik, J., Bosiacki, J., Cusumano, Z., Jensen, C., Willumsen, N., Karsdal, M. A., Liu, L., Langermann, S., Willems, S., Flies, D. & Meyaard, L. Cancer immunotherapy by NC410, a LAIR-2 Fc protein blocking human LAIR-collagen interaction. *eLife* **10,** e62927 (2021).
19. Horn, L. A., Chariou, P. L., Gameiro, S. R., Qin, H., Iida, M., Fousek, K., Meyer, T. J., Cam, M., Flies, D., Langermann, S., Schlom, J. & Palena, C. Remodeling the tumor microenvironment via blockade of LAIR-1 and TGF-β signaling enables PD-L1–mediated tumor eradication. *J. Clin. Invest.* **132,** e155148 (2022).
20. Xie, J., Gui, X., Deng, M., Chen, H., Chen, Y., Liu, X., Ku, Z., Tan, L., Huang, R., He, Y., Zhang, B., Lewis, C., Chen, K., Xu, L., Xu, J., Huang, T., Liao, X. C., Zhang, N., An, Z. & Zhang, C. C. Blocking LAIR1 signaling in immune cells inhibits tumor development. *Front. Immunol.* **13,** 996026 (2022).

21. Gentles, A. J., Newman, A. M., Liu, C. L., Bratman, S. V., Feng, W., Kim, D., Nair, V. S., Xu, Y., Khuong, A., Hoang, C. D., Diehn, M., West, R. B., Plevritis, S. K. & Alizadeh, A. A. The prognostic landscape of genes and infiltrating immune cells across human cancers. *Nat. Med.* **21,** 938–945 (2015).
22. Fridman, W. H., Galon, J., Dieu-Nosjean, M.-C., Cremer, I., Fisson, S., Damotte, D., Pagès, F., Tartour, E. & Sautès-Fridman, C. in *Cancer Immunol. Immunother.* (ed. Dranoff, G.) **344,** 1–24 (Springer Berlin Heidelberg, 2010).
23. Poh, A. R. & Ernst, M. Targeting Macrophages in Cancer: From Bench to Bedside. *Front. Oncol.* **8,** 49 (2018).
24. Cassetta, L. & Pollard, J. W. Targeting macrophages: therapeutic approaches in cancer. *Nat. Rev. Drug Discov.* **17,** 887–904 (2018).
25. Sarhan, D., Eisinger, S., He, F., Bergsland, M., Pelicano, C., Driescher, C., Westberg, K., Benitez, I. I., Hamoud, R., Palano, G., Li, S., Carannante, V., Muhr, J., Önfelt, B., Schlisio, S., Ravetch, J. V., Heuchel, R., Löhr, M. J. & Karlsson, M. C. I. Targeting myeloid suppressive cells revives cytotoxic anti-tumor responses in pancreatic cancer. *iScience* **25,** 105317 (2022).
26. La Fleur, L., Botling, J., He, F., Pelicano, C., Zhou, C., He, C., Palano, G., Mezheyeuski, A., Micke, P., Ravetch, J. V., Karlsson, M. C. I. & Sarhan, D. Targeting MARCO and IL37R on Immunosuppressive Macrophages in Lung Cancer Blocks Regulatory T Cells and Supports Cytotoxic Lymphocyte Function. *Cancer Res.* **81,** 956–967 (2021).
27. Georgoudaki, A.-M., Prokopec, K. E., Boura, V. F., Hellqvist, E., Sohn, S., Östling, J., Dahan, R., Harris, R. A., Rantalainen, M., Klevebring, D., Sund, M., Brage, S. E., Fuxe, J., Rolny, C., Li, F., Ravetch, J. V. & Karlsson, M. C. I. Reprogramming Tumor-Associated Macrophages by Antibody Targeting Inhibits Cancer Progression and Metastasis. *Cell Rep.* **15,** 2000–2011 (2016).
28. La Fleur, L., Boura, V. F., Alexeyenko, A., Berglund, A., Pontén, V., Mattsson, J. S. M., Djureinovic, D., Persson, J., Brunnström, H., Isaksson, J., Brandén, E., Koyi, H., Micke, P., Karlsson, M. C. I. & Botling, J. Expression of scavenger receptor MARCO defines a targetable tumor-associated macrophage subset in non-small cell lung cancer. *Int. J. Cancer* **143,** 1741–1752 (2018).
29. Lundgren, S., Karnevi, E., Elebro, J., Nodin, B., Karlsson, M. C. I., Eberhard, J., Leandersson, K. & Jirström, K. The clinical importance of tumour-infiltrating macrophages and dendritic cells in periampullary adenocarcinoma differs by morphological subtype. *J. Transl. Med.* **15,** 152 (2017).
30. Movita, D., Kreefft, K., Biesta, P., van Oudenaren, A., Leenen, P. J. M., Janssen, H. L. A. & Boonstra, A. Kupffer cells express a unique combination of phenotypic and functional characteristics compared with splenic and peritoneal macrophages. *J. Leukoc. Biol.* **92,** 723–733 (2012).
31. Arredouani, M. S., Palecanda, A., Koziel, H., Huang, Y.-C., Imrich, A., Sulahian, T. H., Ning, Y. Y., Yang, Z., Pikkarainen, T., Sankala, M., Vargas, S. O., Takeya, M., Tryggvason, K. & Kobzik,

L. MARCO Is the Major Binding Receptor for Unopsonized Particles and Bacteria on Human Alveolar Macrophages. *J. Immunol.* **175,** 6058–6064 (2005).

32. PrabhuDas, M. R., Baldwin, C. L., Bollyky, P. L., Bowdish, D. M. E., Drickamer, K., Febbraio, M., Herz, J., Kobzik, L., Krieger, M., Loike, J., McVicker, B., Means, T. K., Moestrup, S. K., Post, S. R., Sawamura, T., Silverstein, S., Speth, R. C., Telfer, J. C., Thiele, G. M., Wang, X.-Y., Wright, S. D. & El Khoury, J. A Consensus Definitive Classification of Scavenger Receptors and Their Roles in Health and Disease. *J. Immunol.* **198,** 3775–3789 (2017).
33. van der Laan, L. J. W., Döpp, E. A., Haworth, R., Pikkarainen, T., Kangas, M., Elomaa, O., Dijkstra, C. D., Gordon, S., Tryggvason, K. & Kraal, G. Regulation and Functional Involvement of Macrophage Scavenger Receptor MARCO in Clearance of Bacteria In Vivo. *J. Immunol.* **162,** 939–947 (1999).
34. Murthy, S., Larson-Casey, J. L., Ryan, A. J., He, C., Kobzik, L. & Carter, A. B. Alternative activation of macrophages and pulmonary fibrosis are modulated by scavenger receptor, macrophage receptor with collagenous structure. *FASEB J.* **29,** 3527–3536 (2015).
35. Yang, L.-L., Zhang, M.-J., Wu, L., Mao, L., Chen, L., Yu, G.-T., Deng, W.-W., Zhang, W.-F., Liu, B., Sun, W.-K. & Sun, Z.-J. LAIR-1 overexpression and correlation with advanced pathological grade and immune suppressive status in oral squamous cell carcinoma. *Head Neck* **41,** 1080–1086 (2019).
36. Novakowski, K. E., Huynh, A., Han, S., Dorrington, M. G., Yin, C., Tu, Z., Pelka, P., Whyte, P., Guarné, A., Sakamoto, K. & Bowdish, D. M. E. A naturally occurring transcript variant of MARCO reveals the SRCR domain is critical for function. *Immunol. Cell Biol.* **94,** 646–655 (2016).
37. Brondijk, T. H. C., De Ruiter, T., Ballering, J., Wienk, H., Lebbink, R. J., Van Ingen, H., Boelens, R., Farndale, R. W., Meyaard, L. & Huizinga, E. G. Crystal structure and collagen-binding site of immune inhibitory receptor LAIR-1: unexpected implications for collagen binding by platelet receptor GPVI. *Blood* **115,** 1364–1373 (2010).
38. Chanput, W., Mes, J. J. & Wichers, H. J. THP-1 cell line: An in vitro cell model for immune modulation approach. *Int. Immunopharmacol.* **23,** 37–45 (2014).
39. Lambrechts, D., Wauters, E., Boeckx, B., Aibar, S., Nittner, D., Burton, O., Bassez, A., Decaluwé, H., Pircher, A., Van den Eynde, K., Weynand, B., Verbeken, E., De Leyn, P., Liston, A., Vansteenkiste, J., Carmeliet, P., Aerts, S. & Thienpont, B. Phenotype molding of stromal cells in the lung tumor microenvironment. *Nat. Med.* **24,** 1277–1289 (2018).
40. Chan, J. M., Quintanal-Villalonga, Á., Gao, V. R., Xie, Y., Allaj, V., Chaudhary, O., Masilionis, I., Egger, J., Chow, A., Walle, T., Mattar, M., Yarlagadda, D. V. K., Wang, J. L., Uddin, F., Offin, M., Ciampricotti, M., Qeriqi, B., Bahr, A., de Stanchina, E., Bhanot, U. K., Lai, W. V., Bott, M. J., Jones, D. R., Ruiz, A., Baine, M. K., Li, Y., Rekhtman, N., Poirier, J. T., Nawy, T., Sen, T., Mazutis, L., Hollmann, T. J., Pe'er, D. & Rudin, C. M. Signatures of plasticity, metastasis, and immunosuppression in an atlas of human small cell lung cancer. *Cancer Cell* **39,** 1479-1496.e18 (2021).

41. Leader, A. M., Grout, J. A., Maier, B. B., Nabet, B. Y., Park, M. D., Tabachnikova, A., Chang, C., Walker, L., Lansky, A., Le Berichel, J., Troncoso, L., Malissen, N., Davila, M., Martin, J. C., Magri, G., Tuballes, K., Zhao, Z., Petralia, F., Samstein, R., D'Amore, N. R., Thurston, G., Kamphorst, A. O., Wolf, A., Flores, R., Wang, P., Müller, S., Mellman, I., Beasley, M. B., Salmon, H., Rahman, A. H., Marron, T. U., Kenigsberg, E. & Merad, M. Single-cell analysis of human non-small cell lung cancer lesions refines tumor classification and patient stratification. *Cancer Cell* **39,** 1594-1609.e12 (2021).
42. Zilionis, R., Engblom, C., Pfirschke, C., Savova, V., Zemmour, D., Saatcioglu, H. D., Krishnan, I., Maroni, G., Meyerovitz, C. V., Kerwin, C. M., Choi, S., Richards, W. G., De Rienzo, A., Tenen, D. G., Bueno, R., Levantini, E., Pittet, M. J. & Klein, A. M. Single-Cell Transcriptomics of Human and Mouse Lung Cancers Reveals Conserved Myeloid Populations across Individuals and Species. *Immunity* **50,** 1317-1334.e10 (2019).
43. Sade-Feldman, M., Yizhak, K., Bjorgaard, S. L., Ray, J. P., de Boer, C. G., Jenkins, R. W., Lieb, D. J., Chen, J. H., Frederick, D. T., Barzily-Rokni, M., Freeman, S. S., Reuben, A., Hoover, P. J., Villani, A.-C., Ivanova, E., Portell, A., Lizotte, P. H., Aref, A. R., Eliane, J.-P., Hammond, M. R., Vitzthum, H., Blackmon, S. M., Li, B., Gopalakrishnan, V., Reddy, S. M., Cooper, Z. A., Paweletz, C. P., Barbie, D. A., Stemmer-Rachamimov, A., Flaherty, K. T., Wargo, J. A., Boland, G. M., Sullivan, R. J., Getz, G. & Hacohen, N. Defining T Cell States Associated with Response to Checkpoint Immunotherapy in Melanoma. *Cell* **175,** 998-1013.e20 (2018).
44. Wu, S. Z., Al-Eryani, G., Roden, D. L., Junankar, S., Harvey, K., Andersson, A., Thennavan, A., Wang, C., Torpy, J. R., Bartonicek, N., Wang, T., Larsson, L., Kaczorowski, D., Weisenfeld, N. I., Uytingco, C. R., Chew, J. G., Bent, Z. W., Chan, C.-L., Gnanasambandapillai, V., Dutertre, C.-A., Gluch, L., Hui, M. N., Beith, J., Parker, A., Robbins, E., Segara, D., Cooper, C., Mak, C., Chan, B., Warrier, S., Ginhoux, F., Millar, E., Powell, J. E., Williams, S. R., Liu, X. S., O'Toole, S., Lim, E., Lundeberg, J., Perou, C. M. & Swarbrick, A. A single-cell and spatially resolved atlas of human breast cancers. *Nat. Genet.* **53,** 1334–1347 (2021).
45. Azizi, E., Carr, A. J., Plitas, G., Cornish, A. E., Konopacki, C., Prabhakaran, S., Nainys, J., Wu, K., Kiseliovas, V., Setty, M., Choi, K., Fromme, R. M., Dao, P., McKenney, P. T., Wasti, R. C., Kadaveru, K., Mazutis, L., Rudensky, A. Y. & Pe'er, D. Single-Cell Map of Diverse Immune Phenotypes in the Breast Tumor Microenvironment. *Cell* **174,** 1293-1308.e36 (2018).
46. Meyaard, L., Hurenkamp, J., Clevers, H., Lanier, L. L. & Phillips, J. H. Leukocyte-Associated Ig-Like Receptor-1 Functions as an Inhibitory Receptor on Cytotoxic T Cells. *J. Immunol.* **162,** 5800–5804 (1999).
47. Meyaard, L. The inhibitory collagen receptor LAIR-1 (CD305). *J. Leukoc. Biol.* **83,** 799–803 (2008).
48. Mukhopadhyay, S., Chen, Y., Sankala, M., Peiser, L., Pikkarainen, T., Kraal, G., Tryggvason, K. & Gordon, S. MARCO, an innate activation marker of macrophages, is a class A scavenger receptor for Neisseria meningitidis. *Eur. J. Immunol.* **36,** 940–949 (2006).
49. van der Laan, L. J. W., Döpp, E. A., Haworth, R., Pikkarainen, T., Kangas, M., Elomaa, O., Dijkstra, C. D., Gordon, S., Tryggvason, K. & Kraal, G. Regulation and Functional Involvement

of Macrophage Scavenger Receptor MARCO in Clearance of Bacteria In Vivo. *J. Immunol.* **162,** 939–947 (1999).

50. Weinstein, J. N., Collisson, E. A., Mills, G. B., Shaw, K. M., Ozenberger, B. A., Ellrott, K., Shmulevich, I., Sander, C. & Stuart, J. M. The Cancer Genome Atlas Pan-Cancer Analysis Project. *Nat. Genet.* **45,** 1113–1120 (2013).
51. Rumpret, M., von Richthofen, H. J., Peperzak, V. & Meyaard, L. Inhibitory pattern recognition receptors. *J. Exp. Med.* **219,** e20211463 (2022).
52. Ohtani, K., Suzuki, Y., Eda, S., Kawai, T., Kase, T., Keshi, H., Sakai, Y., Fukuoh, A., Sakamoto, T., Itabe, H., Suzutani, T., Ogasawara, M., Yoshida, I. & Wakamiya, N. The Membrane-type Collectin CL-P1 Is a Scavenger Receptor on Vascular Endothelial Cells. *J. Biol. Chem.* **276,** 44222–44228 (2001).
53. Forteza, R. M., Casalino-Matsuda, S. M., Falcon, N. S., Valencia Gattas, M. & Monzon, M. E. Hyaluronan and Layilin Mediate Loss of Airway Epithelial Barrier Function Induced by Cigarette Smoke by Decreasing E-cadherin. *J. Biol. Chem.* **287,** 42288–42298 (2012).
54. Bäumer, D., Lee, S., Nicholson, G., Davies, J. L., Parkinson, N. J., Murray, L. M., Gillingwater, T. H., Ansorge, O., Davies, K. E. & Talbot, K. Alternative Splicing Events Are a Late Feature of Pathology in a Mouse Model of Spinal Muscular Atrophy. *PLoS Genet.* **5,** e1000773 (2009).
55. Sugiura, D., Maruhashi, T., Okazaki, I. M., Shimizu, K., Maeda, T. K., Takemoto, T. & Okazaki, T. Restriction of PD-1 function by cis-PD-L1/CD80 interactions is required for optimal T cell responses. *Science* **364,** 558–566 (2019).
56. Collins, B. E., Blixt, O., Han, S., Duong, B., Li, H., Nathan, J. K., Bovin, N. & Paulson, J. C. High-Affinity Ligand Probes of CD22 Overcome the Threshold Set by *cis* Ligands to Allow for Binding, Endocytosis, and Killing of B Cells. *J. Immunol.* **177,** 2994–3003 (2006).
57. Mori, Y., Tsuji, S., Inui, M., Sakamoto, Y., Endo, S., Ito, Y., Fujimura, S., Koga, T., Nakamura, A., Takayanagi, H., Itoi, E. & Takai, T. Inhibitory Immunoglobulin-Like Receptors LILRB and PIR-B Negatively Regulate Osteoclast Development. *J. Immunol.* **181,** 4742–4751 (2008).
58. Davis, S. J. & Van Der Merwe, P. A. The kinetic-segregation model: TCR triggering and beyond. *Nat. Immunol.* **7,** 803–809 (2006).
59. Murray, P. J., Allen, J. E., Biswas, S. K., Fisher, E. A., Gilroy, D. W., Goerdt, S., Gordon, S., Hamilton, J. A., Ivashkiv, L. B., Lawrence, T., Locati, M., Mantovani, A., Martinez, F. O., Mege, J.-L., Mosser, D. M., Natoli, G., Saeij, J. P., Schultze, J. L., Shirey, K. A., Sica, A., Suttles, J., Udalova, I., van Ginderachter, J. A., Vogel, S. N. & Wynn, T. A. Macrophage Activation and Polarization: Nomenclature and Experimental Guidelines. *Immunity* **41,** 14–20 (2014).
60. Schultz, H. S., Guo, L., Keller, P., Fleetwood, A. J., Sun, M., Guo, W., Ma, C., Hamilton, J. A., Bjørkdahl, O., Berchtold, M. W. & Panina, S. OSCAR-collagen signaling in monocytes plays a proinflammatory role and may contribute to the pathogenesis of rheumatoid arthritis. *Eur. J. Immunol.* **46,** 952–963 (2016).
61. Eisinger, S., Sarhan, D., Boura, V. F., Ibarlucea-Benitez, I., Tyystjärvi, S., Oliynyk, G., Arsenian-Henriksson, M., Lane, D., Wikström, S. L., Kiessling, R., Virgilio, T., Gonzalez, S. F., Kaczynska, D., Kanatani, S., Daskalaki, E., Wheelock, C. E., Sedimbi, S., Chambers, B. J., Ravetch, J. V. &

Karlsson, M. C. I. Targeting a scavenger receptor on tumor-associated macrophages activates tumor cell killing by natural killer cells. *Proc. Natl. Acad. Sci.* **117,** 32005–32016 (2020).

62. Rumpret, M., Richthofen, H. J., Linden, M., Westerlaken, G. H. A., Talavera Ormeño, C., Low, T. Y., Ovaa, H. & Meyaard, L. Recognition of S100 proteins by Signal Inhibitory Receptor on Leukocytes-1 negatively regulates human neutrophils. *Eur. J. Immunol.* **51,** 2210–2217 (2021).
63. Niederauer, C., Seynen, M., Zomerdijk, J., Kamp, M. & Ganzinger, K. A. The K2: Open-source simultaneous triple-color TIRF microscope for live-cell and single-molecule imaging. *HardwareX* **13,** (2023).
64. Niederauer, C., Wang-Henderson, M. & Escoffier, E. SPIT. (2022). at <https://github.com/GanzingerLab/SPIT>
65. Davie, K., De Waegeneer, M. & Kreft, Ł. SCope v1.8.2: Visualization of large-scale and high dimensional single cell data. (2023). at <https://github.com/aertslab/SCope>
66. Chan JM, Quintanal-Villalonga Á, Gao VR, Xie Y, Allaj V, Chaudhary O, Masilionis I, Egger J, Chow A, Walle T, Mattar M, Yarlagadda DVK, Wang JL, Uddin F, Offin M, Ciampricotti M, Qeriqi B, Bahr A, de Stanchina E, Bhanot UK, Lai WV, Bott MJ, Jones DR, Ruiz A, Baine MK, Li Y, Rekhtman N, Poirier JT, Nawy T, Sen T, Mazutis L, Hollmann TJ, Pe'er D, Rudin CM. Signatures of plasticity, metastasis, and immunosuppression in an atlas of human small cell lung cancer. *Cancer Cell.* **39**, 1479-1496.e18 (2021).

Acknowledgments: We thank A. Ashique, J. Furneisen, and J. Tian for their contributions to the work in this study, L. Lavis for the generous gift of the Janelia Fluor dyes, and D. Bowdish and E. de Jong for the MARCO and MARCOII expression vectors.

Funding: Part of this work was supported by Dutch Cancer Society/KWF grant #14339. N.J. is supported by the Human Frontier Science Program Long-Term Postdoctoral Fellowship (LT 0031/2023-L) and EMBO Postdoctoral Fellowship (ALTF 896-2022).

Author contributions: Conceptualization and study design: A.S., S.V.V., J. Sissons, J. Sitrin, M.I.P.R., and L.M. Methodology: A.S., S.V.V., H.A.-T., and N.J. Performing experiments and data analysis: A.S., S.V.V., H.A,-T., N.J., P.C., S.C., K.M., J.Z., C.N., Z.M., B.L., and B.F. Project management and supervision: M.v.d.V., D.D.K., L.B.R., J. Sissons, J. Sitrin, K.A.G., M.I.P.R., and L.M. Writing of the original draft: A.S. and S.V.V. Writing, reviewing and editing: H.A,-T., N.J., M.v.d.V., D.D.K., L.B.R., J. Sissons, J. Sitrin, K.A.G., M.I.P.R., and L.M.

Competing interests: P.C., S.C., K.M., J.Z., Z.M., B.L., B.F., D.D.K., L.B.R., J. Sissons, and J. Sitrin are employees of NGM Biopharmaceuticals Inc. S.C., B.L., B.F., L.B.R, J. Sissons, and J. Sitrin are inventors on a patent regarding LAIR-1-binding agents and methods of use thereof (international publication number WO 2021/262597 A2). The research lab of L.M. has received financial support for investigator-initiated studies on LAIR-1 from Boehringer Ingelheim, NextCure, and NGM Biopharmaceuticals, all paid to institute. Part of the work in this study was supported by NGM Biopharmaceuticals Inc. The other authors declare that they have no competing interests.

Data and materials availability: The data underlying Figs. 2 and 6 are available in the Gene Expression Omnibus (GSE114725, GSE176078, GSE120575, GSE127465, and GSE154826) and online (https://scope.aertslab.org/#/Bernard_Thienpont/*/welcome; Chan *et al.* 2021[66] and https://portal.gdc.cancer.gov/). All other data needed to evaluate the conclusions in the paper are present in the paper or the Supplementary Materials. Some materials used in this study are subject to a materials transfer agreement (MTA) or can only be distributed under an MTA. Further information and requests for resources and reagents should be directed to L.M.

Fig. 1. MARCO is a previously uncharacterized functional ligand for LAIR-1. (**A**) Immunofluorescence staining of control and MARCO-expressing transfected HEK293T cells using LAIR-1-Fc fusion protein. (**B**) Binding of LAIR-1-Fc fusion protein to parental, MARCO- and Coll-XVII-expressing transfected K562 cells as determined by flow cytometry. (**C**) Affinity measurements of MARCO and collagen I to immobilized LAIR-1-Fc as determined by SPR analysis. The concentrations of collagen I and MARCO ranged from 6.25 to 200 nM. (**D**) Real-time binding signal from two parallel sensors obtained by the Octet, HTX platform. In the absence of MARCO (step 3, blue trace), collagen I showed high binding to LAIR-1 (step 4, blue trace), which was reduced by pre-binding MARCO to LAIR-1 (step 4, red trace). (**E** and **F**) Flow cytometry analysis (E) and quantification (F) of LAIR-1-Fc fusion protein binding to parental, MARCO-expressing, and MARCOII-expressing transfected HEK293T cells. Data are from three experiments and were analyzed by Kruskal-Wallis test ($P = 0.05$). (**G**) The indicated antibody controls and recombinant proteins were immobilized on plastic culture plates. After washing, WT, LAIR-1a-CD3ζ, or LAIR-1b-CD3ζ NFAT-GFP 2B4 reporter cells were added and cultured for 18 hours, after which the cells were harvested and assessed for GFP production by flow cytometry. (**H**) WT, MARCO-, collagen XVII–, and CD32-expressing LCL721.221 target cells were co-cultured with WT or LAIR-1-expressing YT.2C2 effector cells at the indicated effector:target (E:T) ratios, and target cell viability was determined by flow cytometry. $CD32^+$ cells were additionally cultured with anti-LAIR-1 antibodies to ligate LAIR-1 on effector cells. Data in (G) and (H) are from three or four experiments and were analyzed with a mixed-effect analysis with Tukey's multiple comparison correction. *$P \leq 0.05$; **$P \leq 0.01$; ****$P \leq 0.0001$.

Fig. 2. LAIR-1 and MARCO are co-expressed on macrophages. (**A**) The percentages of macrophages expressing *LAIR1, MARCO,* or *LAIR1* and *MARCO* in scRNA-seq data obtained from different studies of patients with the indicated cancer types. MEL, melanoma. (**B**) Percentage of *MARCO*-expressing macrophages that also express *LAIR1* in scRNA-seq data from different studies of patients with the indicated cancer types. (**C** and **D**) Human monocytes were isolated from peripheral blood and differentiated to M0 or M2c-like monocyte-derived macrophages (MDMs) with M-CSF alone or in the presence of IL-10, respectively. Flow cytometry analysis of cells from representative donor (C) and quantification of the percentage of live MDMs that co-expressed MARCO and LAIR-1 (D). Data are from six donors in two independent experiments and were analyzed by Wilcoxon test. *$P \leq 0.05$.

Fig. 3. LAIR-1 and MARCO can interact in cis when expressed in the same cell. (**A**) Schematic overview of the TIRF microscopy setup to determine interactions between LAIR-1 and MARCO. Cells expressing LAIR-1, MARCO, or both were allowed to adhere to a PLL-coated glass surface, and fluorescence was measured over time by TIRF microscopy. (**B**) Overview of image acquisition and analysis for TIRF microscopy. Cells expressing high amounts of MARCO and LAIR-1 were selected, and the LAIR-1 signal was photobleached to better track single molecules. Single molecules could then be localized and tracked over time. (**C**) Representative images of MARCO (top) and LAIR-1 (bottom) tracks as determined by single-particle tracking after live-cell TIRF microscopy. The color indicates the time of localization within the timeframe, and the white outline indicates the photobleached area. (**D**) Quantification of jump distances between separate localizations within a single track for LAIR-1 and MARCO in cells expressing each molecule alone. Colored lines indicate the distribution of jump distances of all tracks within a single cell, whereas colored dots indicate the median jump distance of all tracks per cell. The black line indicates the aggregated jump distance data for all cells, and the blue square indicates the median jump distance of all tracks acquired. Larger jump distances indicate higher mobility, whereas shorter jumps are indicative of lower mobility of the receptor. (**E**) Data are presented as described for (D), but the cells co-expressed MARCO and LAIR-1a (left) or MARCO and LAIR-1b (right) and were additionally incubated with medium, an isotype control antibody, or an anti-LAIR-1 (clone 108D10) antibody to block LAIR-1:MARCO binding. Data are from 6 to 12 cells per group and were analyzed by Kruskal-Wallis test with Dunn's multiple comparison correction. *$P \leq 0.05$.

Fig. 4. The cis interaction between LAIR-1 and MARCO can block the binding of LAIR-1 to collagen. (**A**) Phagocytosis of *E. coli*-pHrodo BioParticles by IL-10–polarized human MDMs in the presence or absence of indicated proteins, which can interfere with the LAIR-1:MARCO interaction, was determined by Incucyte live-cell imaging. The cursive medium control is in the absence of *E. coli* BioParticles. Data are aggregated from three independent experiments; experiments with $F(ab')_2$ fragments were performed twice. (**B**) Quantification of phagocytosed *E. coli* BioParticles under the indicated conditions at 3 hours. (**C**) Left: WT (top left) and MARCO-expressing (bottom left) LAIR-1-CD3ζ NFAT-GFP reporter cells were cultured on the indicated amounts of immobilized collagen and GFP response was determined by flow cytometry. Right: Quantification of the GFP response in the indicated cells. Data are aggregated from four independent experiments. (**D**) Left: THP-$1^{LAIR1-/-}$ cells were transduced to express LAIR-1 alone or with MARCO. Right: Collagen IV-FITC binding to LAIR-1 in the presence or absence of MARCO was then determined by flow cytometry. Data are aggregated from three independent experiments. Data in (C) and (D) were analyzed by two-way ANOVA with Tukey's multiple comparison correction. *$P \leq 0.05$; **$P \leq 0.01$; ***$P \leq 0.001$; ****$P \leq 0.0001$. (n=3-4 experiments).

Fig. 5. MARCO co-expression in primary human macrophages impairs collagen-induced, LAIR-1–mediated inhibition of IL-8 production upon LPS exposure. (**A** and **B**) Flow cytometry analysis of the efficiency of knockout of MARCO or LAIR-1 on IL-10–polarized MDMs. For the quantification of all donors, see fig. S3, A to D. (**C**) Measurement of IL-8 secretion by LPS-stimulated MDMs on BSA- or collagen I–coated wells, normalized to the amount of IL-8 in control BSA-coated wells per CRISPR condition. Data are from seven donors in three independent experiments and were analyzed by the Friedman test. (**D**) Inhibition of IL-8 secretion on collagen I–coated as compared to control BSA-coated wells, which was calculated per CRISPR condition. Data are from seven donors in three independent experiments and were analyzed by one-sided Wilcoxon tests. (**E**) Th co-expression of MARCO and LAIR-1 decreases the inhibitory function of LAIR-1 on human macrophages. LAIR-1 can recognize collagens to induce inhibitory signaling in macrophages. However, when MARCO is increased in abundance, for example in M2-like or tumor-associated macrophages, MARCO can interfere with LAIR-1:collagen interactions, and further increase overall macrophage activation. Created in BioRender. Meyaard, L. (2025) https://BioRender.com/nsup4ad.

Fig. 6. Low MARCO and LAIR-1 expression is associated with increased survival in GBM and LUSC. (**A**) Tumor samples from patients with glioblastoma multiforme (GBM) and lung squamous cell carcinoma (LUSC) in the TCGA were stratified based on *MARCO* expression, and *LAIR1* expression in these samples was assessed. ****$P \leq 0.0001$ by unpaired two-tailed *t* test. (**B**) Tumor samples from patients with GBM (left) and LUSC (right) were stratified based on *MARCO* (top) and *LAIR1* (bottom) expression, and overall survival (OS) was determined. Statistically significant differences in survival were determined by log-rank (Mantel-Cox) test and are indicated in each graph. (**C**) Tumor samples from patients with GBM (left) and LUSC (right) were stratified based on *MARCO* and *LAIR1* expression and OS was determined. Statistically significant differences in survival were determined by log-rank (Mantel-Cox) test and are indicated in each graph. The number of patients are indicated in each graph.

Table 1. LAIR-1 reporter cell activity in response to potential LAIR-1 ligands and extracellular matrix components. The reporter cells expressed the indicated LAIR-1 molecules. Data show the maximal percentage of GFP^+ reporter cells in response to the indicated potential ligands. ND, not determined.

	max GFP^+ reporter cells		
	Human LAIR-1	**Cynomolgus LAIR-1**	**Mouse LAIR-1**
Human Coll-I	42.14 ± 2.7	65.7 ± 11.15	35.75 ± 14.35
Human Coll-IV	48.17 ± 3.73	64.75 ± 13.75	57.9
Mouse Coll-I	65	87.4	36.7
Mouse Coll-IV	62.2	65	10.6
MARCO	37.17 ± 4.17	26.9 ± 8	16.8 ± 3.7
Collectin-12 (SCARA4)	63.5 ± 6.4	9.04 ± 3.66	1.74
Mannose-binding lectin	67.5 ± 3.3	1.73 ± 0.22	1.17
Surfactant protein D	21.75 ± 8.65	2 ± 0.7	1.64
C1q	3.64 ± 0.86	1.78 ± 0.14	39.6
Adiponectin	1.34	1.37	1.5
Laminin	1.98	ND	ND
Fibronectin	1.9	ND	ND
MSR1 (SCARA1)	1.94	3.8	1.41
SCARA3	1.79	1.19	1.51
SCARA5	1.41	1.43	1.4

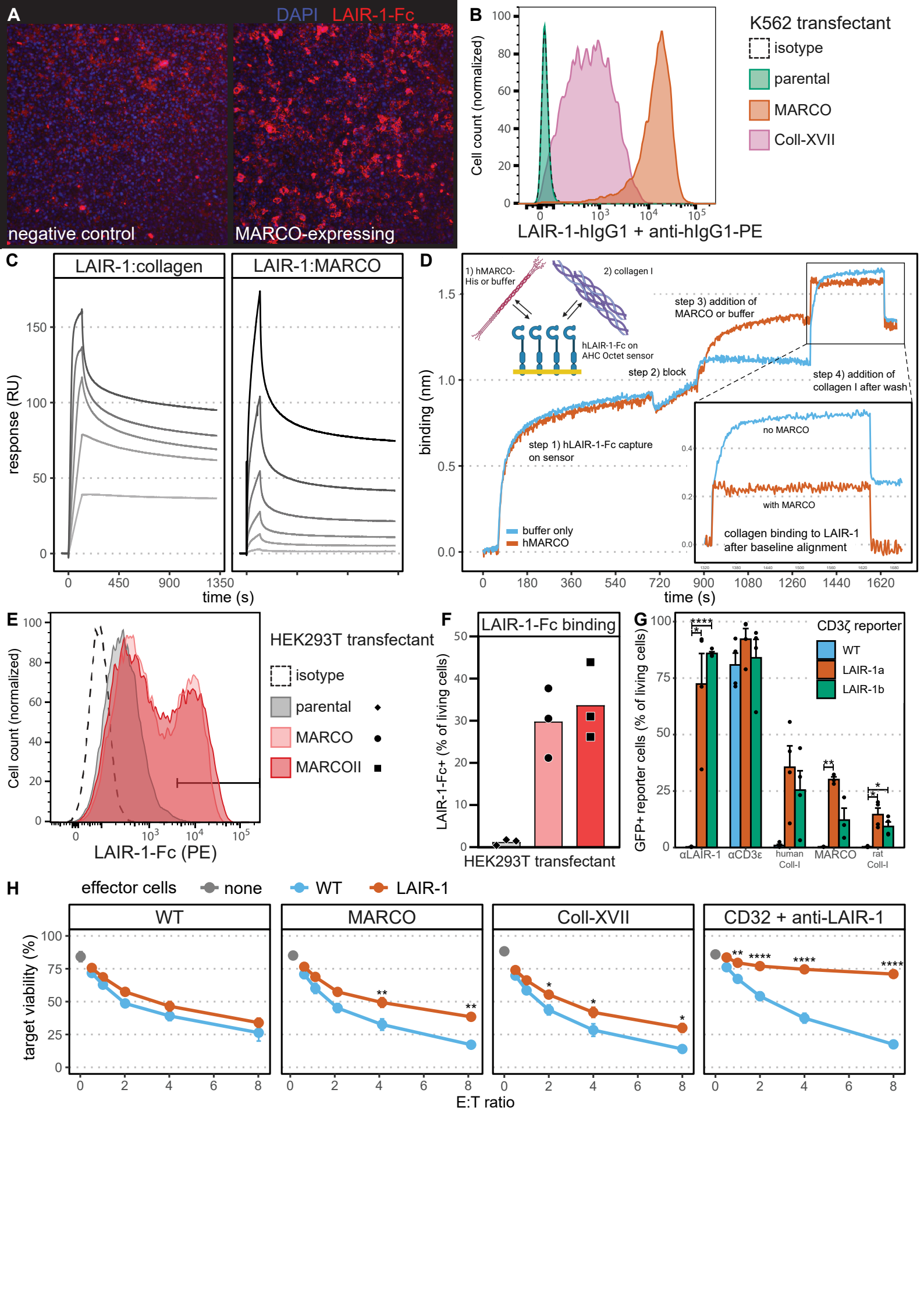
A
DAPI LAIR-1-Fc
negative control
MARCO-expressing
B
Cell count (normalized)
LAIR-1-hIgG1 + anti-hIgG1-PE
K562 transfectant
isotype
parental
MARCO
Coll-XVII
C
LAIR-1:collagen
LAIR-1:MARCO
response (RU)
time (s)
D
1) hMARCO-His or buffer
2) collagen I
hLAIR-1-Fc on AHC Octet sensor
step 1) hLAIR-1-Fc capture on sensor
step 2) block
step 3) addition of MARCO or buffer
step 4) addition of collagen I after wash
buffer only
hMARCO
binding (nm)
time (s)
no MARCO
with MARCO
collagen binding to LAIR-1 after baseline alignment
E
Cell count (normalized)
LAIR-1-Fc (PE)
HEK293T transfectant
isotype
parental
MARCO
MARCOII
F
LAIR-1-Fc binding
LAIR-1-Fc+ (% of living cells)
HEK293T transfectant
G
CD3ζ reporter
WT
LAIR-1a
LAIR-1b
GFP+ reporter cells (% of living cells)
αLAIR-1
αCD3ε
human Coll-I
MARCO
rat Coll-I
H
effector cells
none
WT
LAIR-1
WT
MARCO
Coll-XVII
CD32 + anti-LAIR-1
target viability (%)
E:T ratio

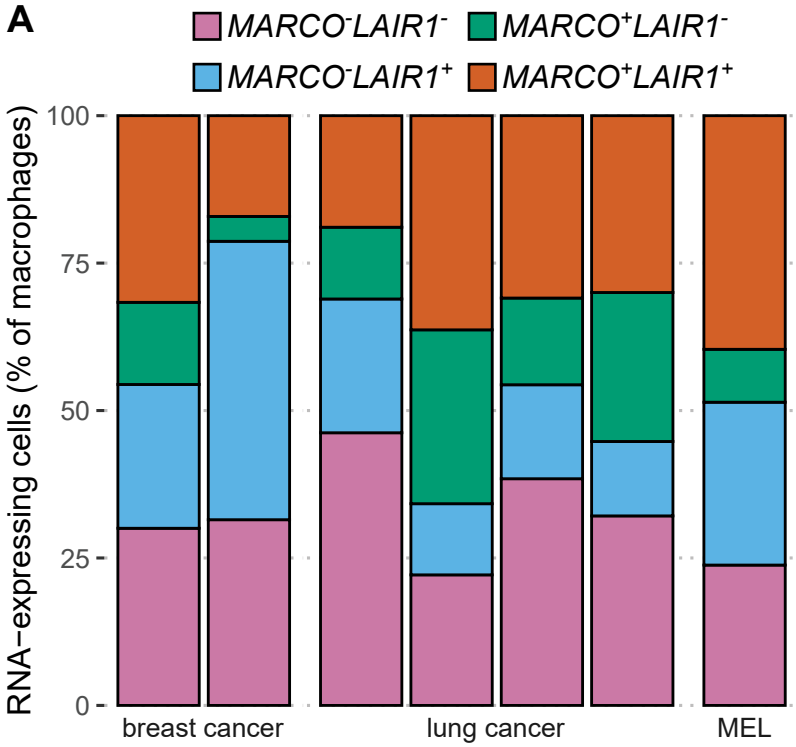
A
MARCO-LAIR1-
MARCO+LAIR1-
MARCO-LAIR1+
MARCO+LAIR1+
RNA−expressing cells (% of macrophages)
100
75
50
25
0
breast cancer
lung cancer
MEL

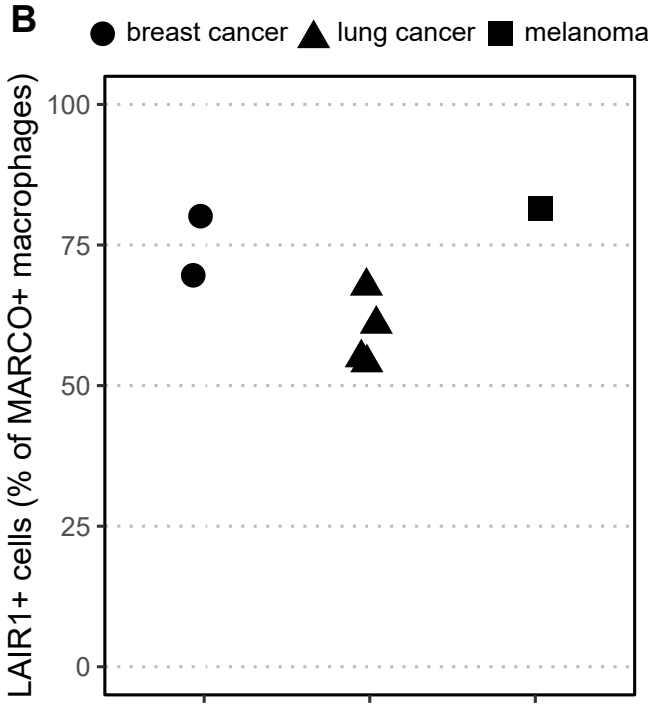
B
breast cancer
lung cancer
melanoma
LAIR1+ cells (% of MARCO+ macrophages)
100
75
50
25
0

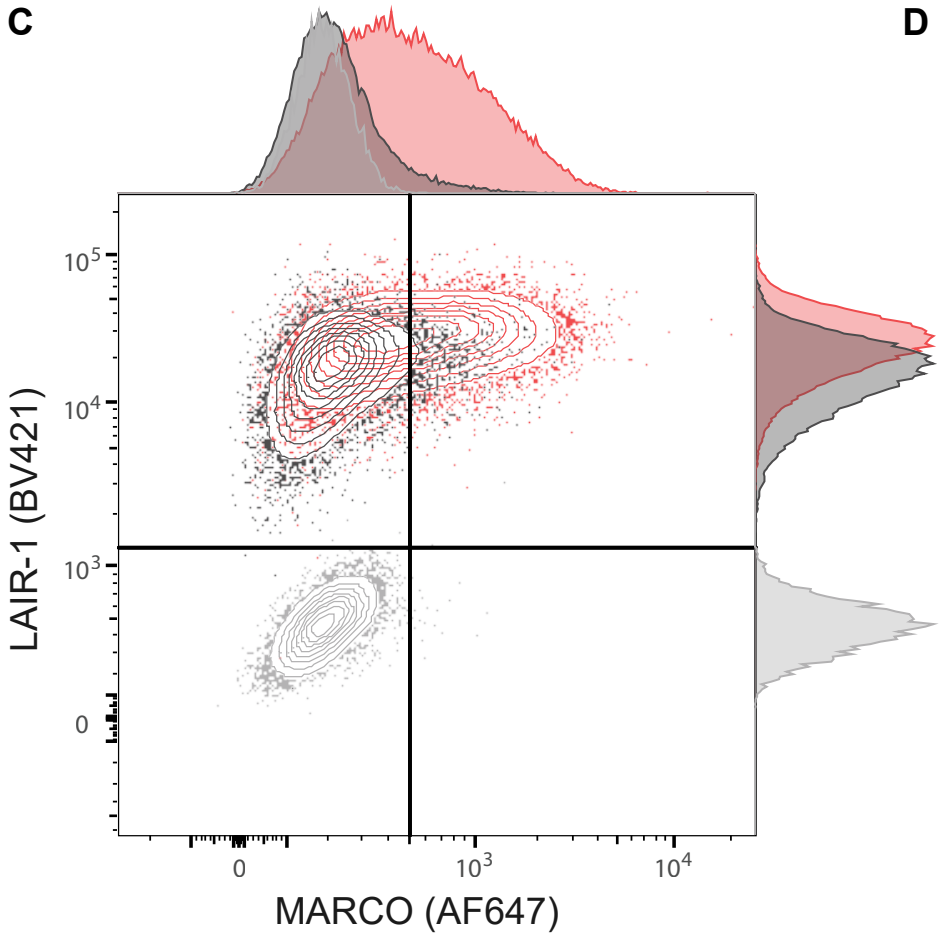
C
LAIR-1 (BV421)
10^5
10^4
10^3
0
0
10^3
10^4
MARCO (AF647)

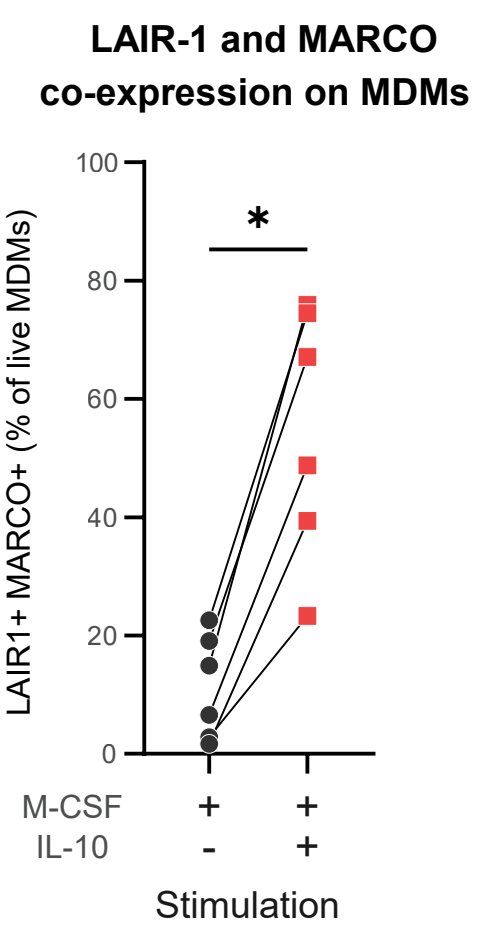
D
LAIR-1 and MARCO
co-expression on MDMs
LAIR1+ MARCO+ (% of live MDMs)
100
80
60
40
20
0
*
M-CSF
IL-10
+
-
+
+
Stimulation

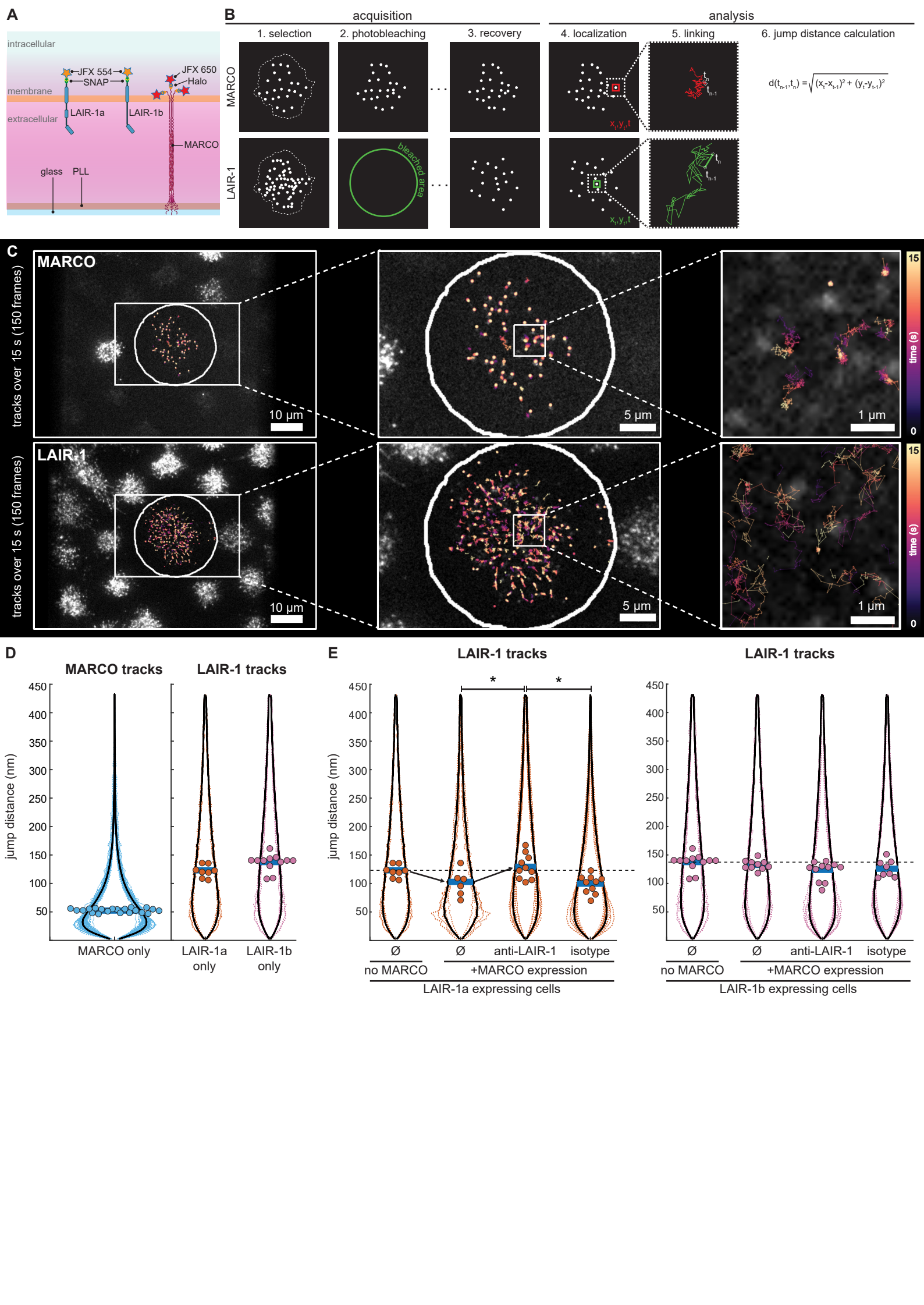
A
intracellular
membrane
extracellular
JFX 554
SNAP
JFX 650
Halo
LAIR-1a
LAIR-1b
MARCO
glass
PLL
B
acquisition
analysis
1. selection
2. photobleaching
3. recovery
4. localization
5. linking
6. jump distance calculation
MARCO
LAIR-1
bleached area
$d(t_{n-1},t_n) = \sqrt{(x_t-x_{t-1})^2 + (y_t-y_{t-1})^2}$
C
MARCO
LAIR-1
tracks over 15 s (150 frames)
10 µm
5 µm
1 µm
time (s)
15
0
D
MARCO tracks
LAIR-1 tracks
jump distance (nm)
450
400
350
300
250
200
150
100
50
MARCO only
LAIR-1a only
LAIR-1b only
E
LAIR-1 tracks
LAIR-1 tracks
*
*
Ø
Ø
anti-LAIR-1
isotype
no MARCO
+MARCO expression
LAIR-1a expressing cells
LAIR-1b expressing cells

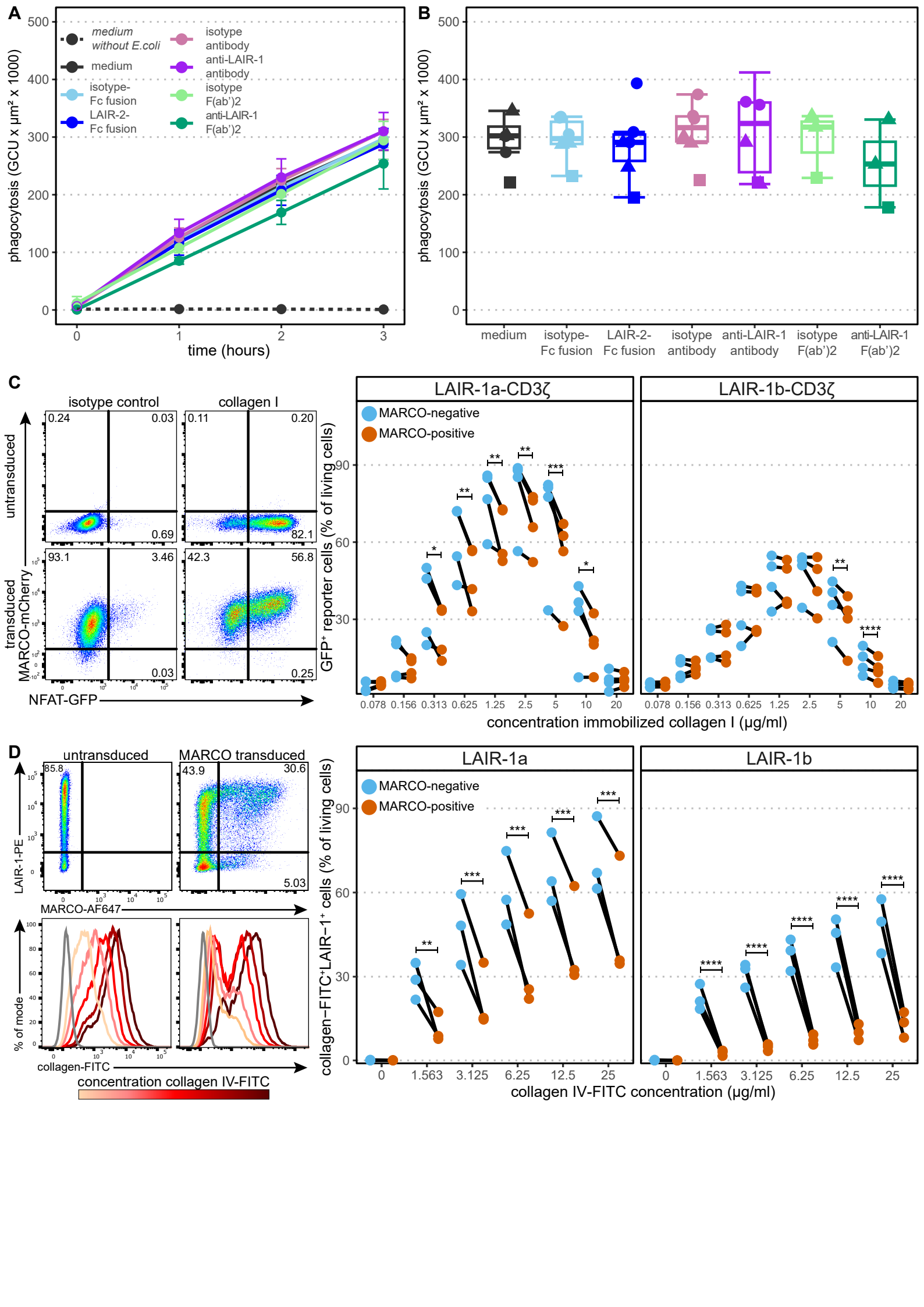
A
phagocytosis (GCU x µm² x 1000)
time (hours)
medium without E.coli
medium
isotype-Fc fusion
LAIR-2-Fc fusion
isotype antibody
anti-LAIR-1 antibody
isotype F(ab')2
anti-LAIR-1 F(ab')2
B
phagocytosis (GCU x µm² x 1000)
medium
isotype-Fc fusion
LAIR-2-Fc fusion
isotype antibody
anti-LAIR-1 antibody
isotype F(ab')2
anti-LAIR-1 F(ab')2
C
isotype control
collagen I
untransduced
transduced MARCO-mCherry
NFAT-GFP
0.24
0.03
0.69
0.11
0.20
82.1
93.1
3.46
0.03
42.3
56.8
0.25
LAIR-1a-CD3ζ
LAIR-1b-CD3ζ
MARCO-negative
MARCO-positive
GFP⁺ reporter cells (% of living cells)
concentration immobilized collagen I (µg/ml)
D
untransduced
MARCO transduced
LAIR-1-PE
MARCO-AF647
85.8
43.9
30.6
5.03
% of mode
collagen-FITC
concentration collagen IV-FITC
LAIR-1a
LAIR-1b
MARCO-negative
MARCO-positive
collagen−FITC⁺LAIR−1⁺ cells (% of living cells)
collagen IV-FITC concentration (µg/ml)

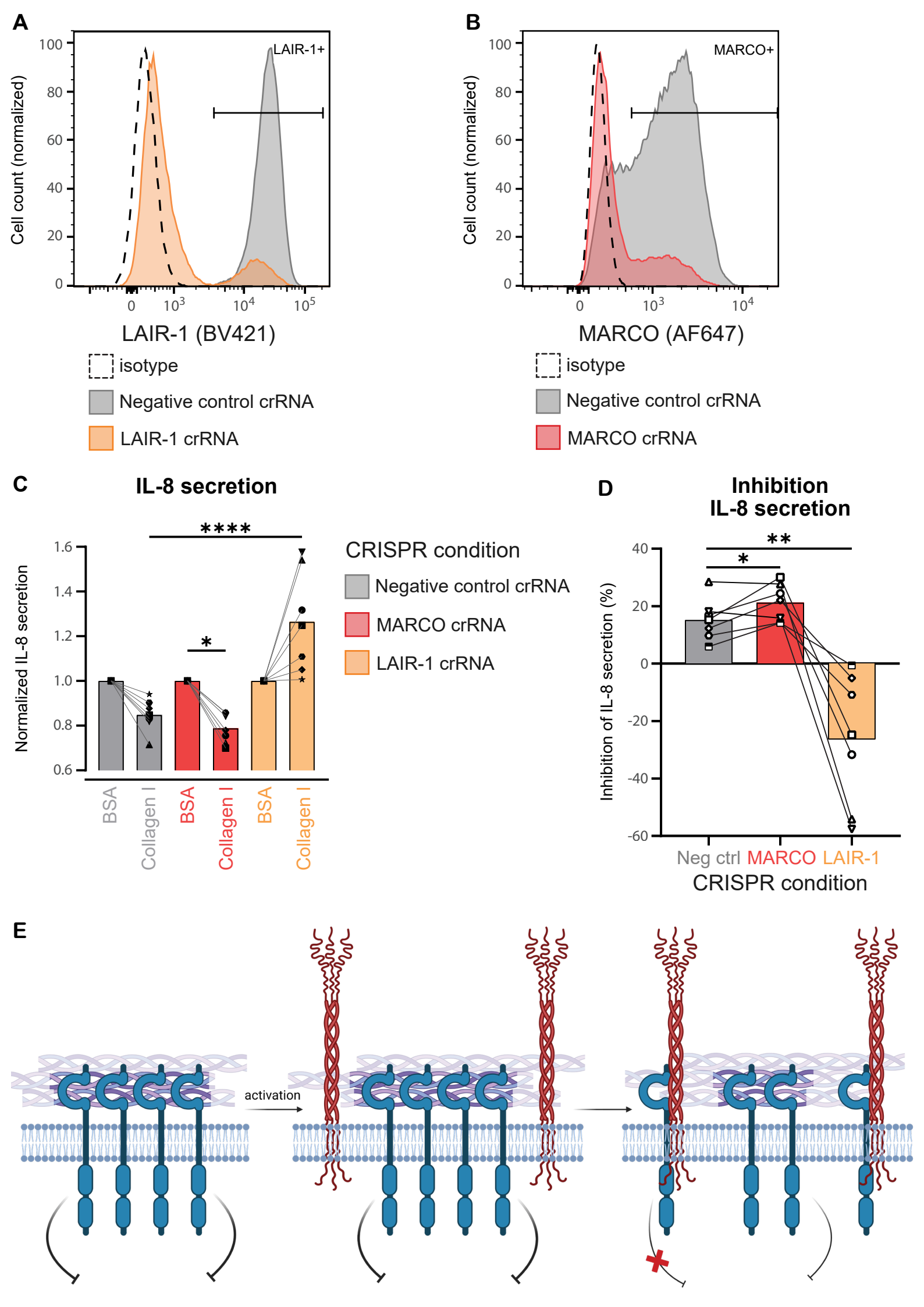
A
LAIR-1+
Cell count (normalized)
LAIR-1 (BV421)
isotype
Negative control crRNA
LAIR-1 crRNA
B
MARCO+
Cell count (normalized)
MARCO (AF647)
isotype
Negative control crRNA
MARCO crRNA
C
IL-8 secretion
****
*
Normalized IL-8 secretion
BSA
Collagen I
BSA
Collagen I
BSA
Collagen I
CRISPR condition
Negative control crRNA
MARCO crRNA
LAIR-1 crRNA
D
Inhibition
IL-8 secretion
**
*
Inhibition of IL-8 secretion (%)
Neg ctrl
MARCO
LAIR-1
CRISPR condition
E
activation

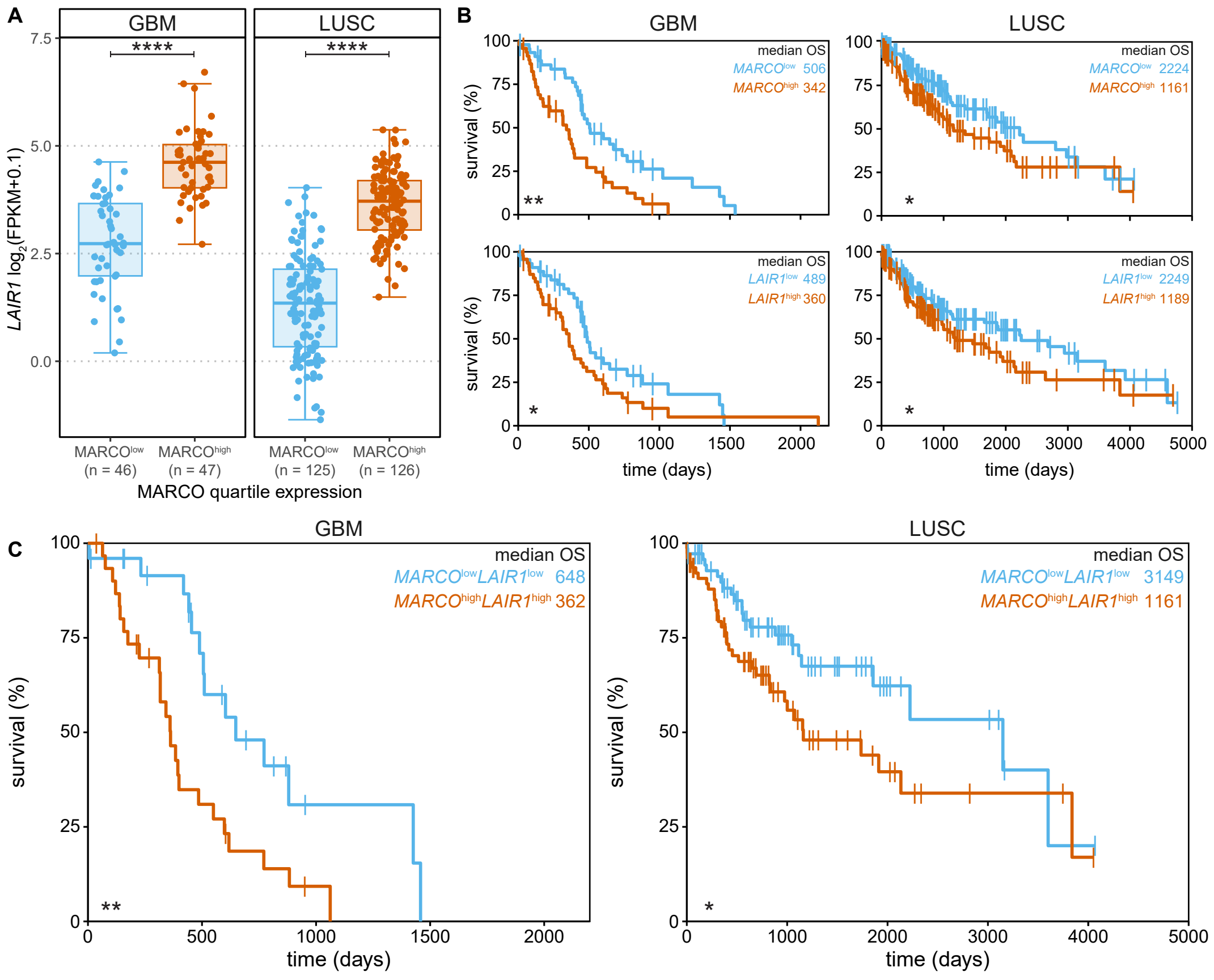
A
GBM
LUSC
****
****
LAIR1 log2(FPKM+0.1)
7.5
5.0
2.5
0.0
MARCOlow (n = 46)
MARCOhigh (n = 47)
MARCOlow (n = 125)
MARCOhigh (n = 126)
MARCO quartile expression
B
GBM
LUSC
median OS
MARCOlow 506
MARCOhigh 342
MARCOlow 2224
MARCOhigh 1161
LAIR1low 489
LAIR1high 360
LAIR1low 2249
LAIR1high 1189
survival (%)
time (days)
C
GBM
LUSC
median OS
MARCOlowLAIR1low 648
MARCOhighLAIR1high 362
MARCOlowLAIR1low 3149
MARCOhighLAIR1high 1161
survival (%)
time (days)

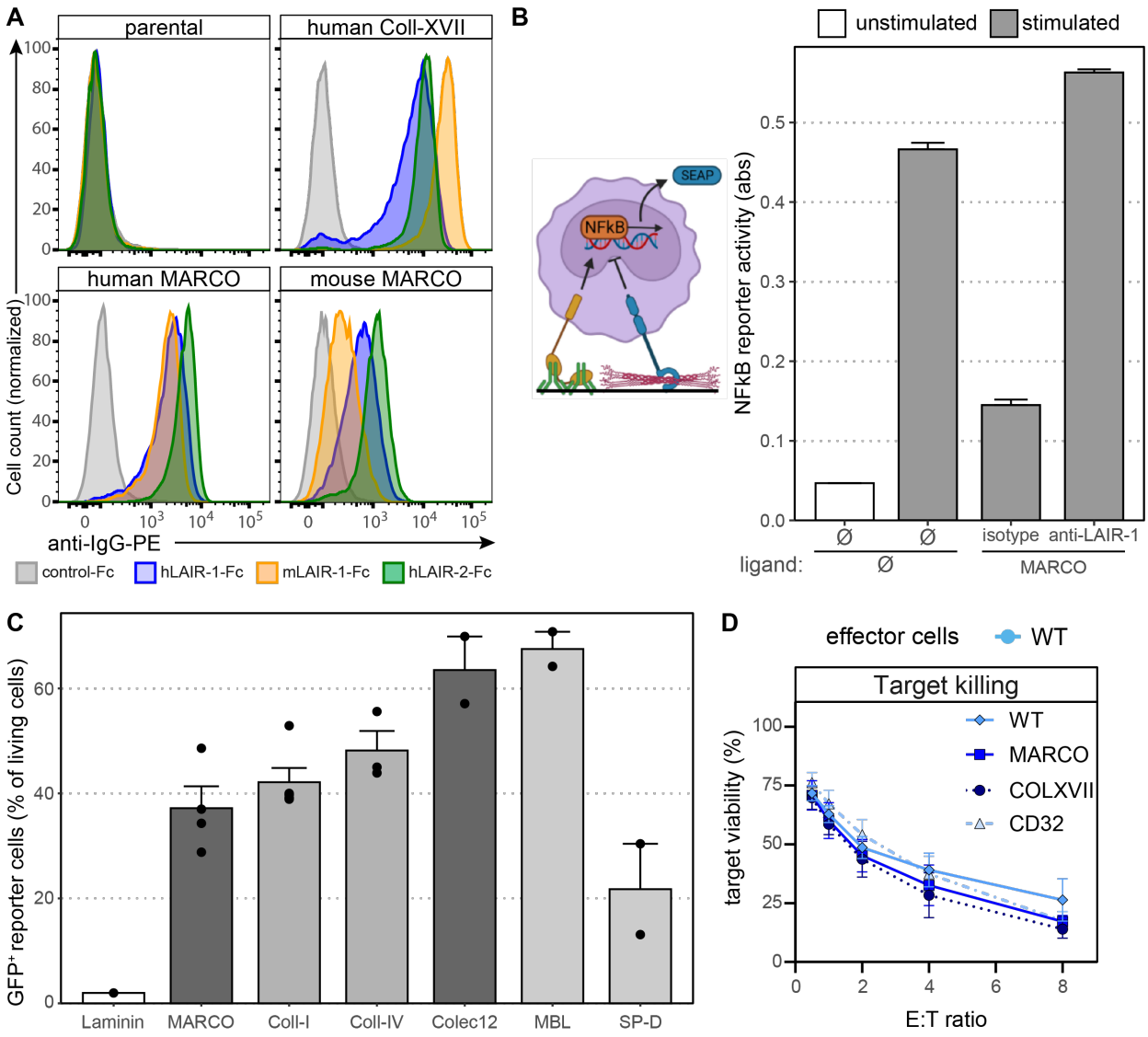

Fig. S1. MARCO is a previously uncharacterized functional ligand for LAIR-1. (**A**) Analysis of the binding of human LAIR-1-Fc, human LAIR-2-Fc, and mouse LAIR-1-Fc fusion proteins to parental, human MARCO-, human collagen XVII-, and mouse MARCO-expressing transduced LCL721.221 cells. (**B**) Left: schematic of the experimental setup. THP-1 NF-κB-SEAP reporter lines were activated through the Fc receptor (orange) with an immobilized antibody (green), resulting in NF-κB-induced SEAP secretion, in the presence or absence of immobilized MARCO (red) as a putative ligand for LAIR-1 (blue) . Right: the NF-κB response was determined in the presence or absence of immobilized MARCO and in the presence of a soluble isotype control antibody or a blocking anti–LAIR-1 antibody. Data are from two experiments with three technical replicates; blocking was performed once. (**C**) The indicated recombinant proteins were immobilized on plastic, and the GFP response of LAIR-1-CD3ζ NFAT-GFP reporter cells was determined after culture. The maximal percentage of GFP^+ reporter cells for each protein is depicted for each experiment. Experiments were performed between one and five times. (**D**) WT, MARCO-, collagen XVII–, and CD32-expressing transfected LCL721.221 target cells were co-cultured with WT YT.2C2 effector cells at the indicated effector:target ratios, and the viability of the target cells was determined by flow cytometry. Data are from three or four experiments.

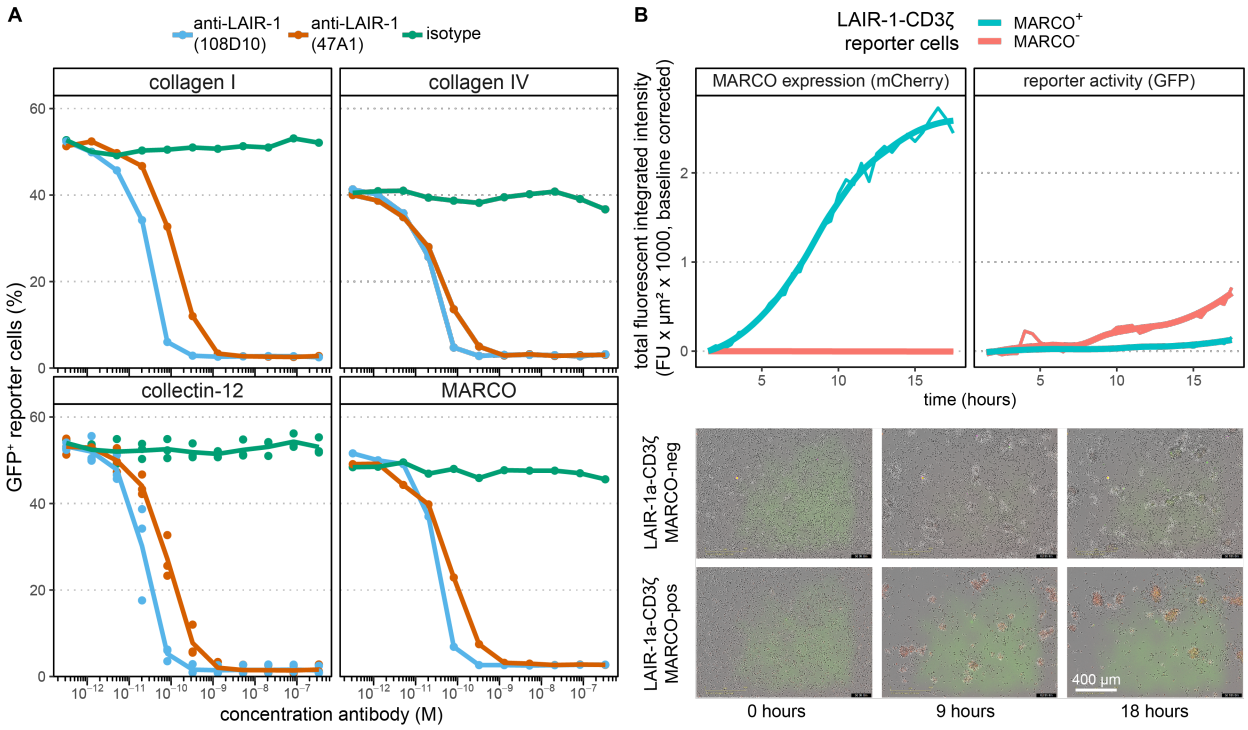

Fig. S2. The cis interaction between LAIR-1 and MARCO can block the binding of LAIR-1 to collagen. (**A**) The indicated proteins were immobilized on plastic and the GFP response of LAIR-1-CD3ζ NFAT-GFP reporter cells was determined in the presence of increasing concentrations of anti-LAIR-1 antibody or isotype control antibody. The data are from one experiment and are representative of three independent experiments. (**B**) LAIR-1-CD3ζ NFAT-GFP reporter cells were left untreated or were transduced to express MARCO-mCherry, and the GFP response was determined over time by Incucyte live-cell imaging.

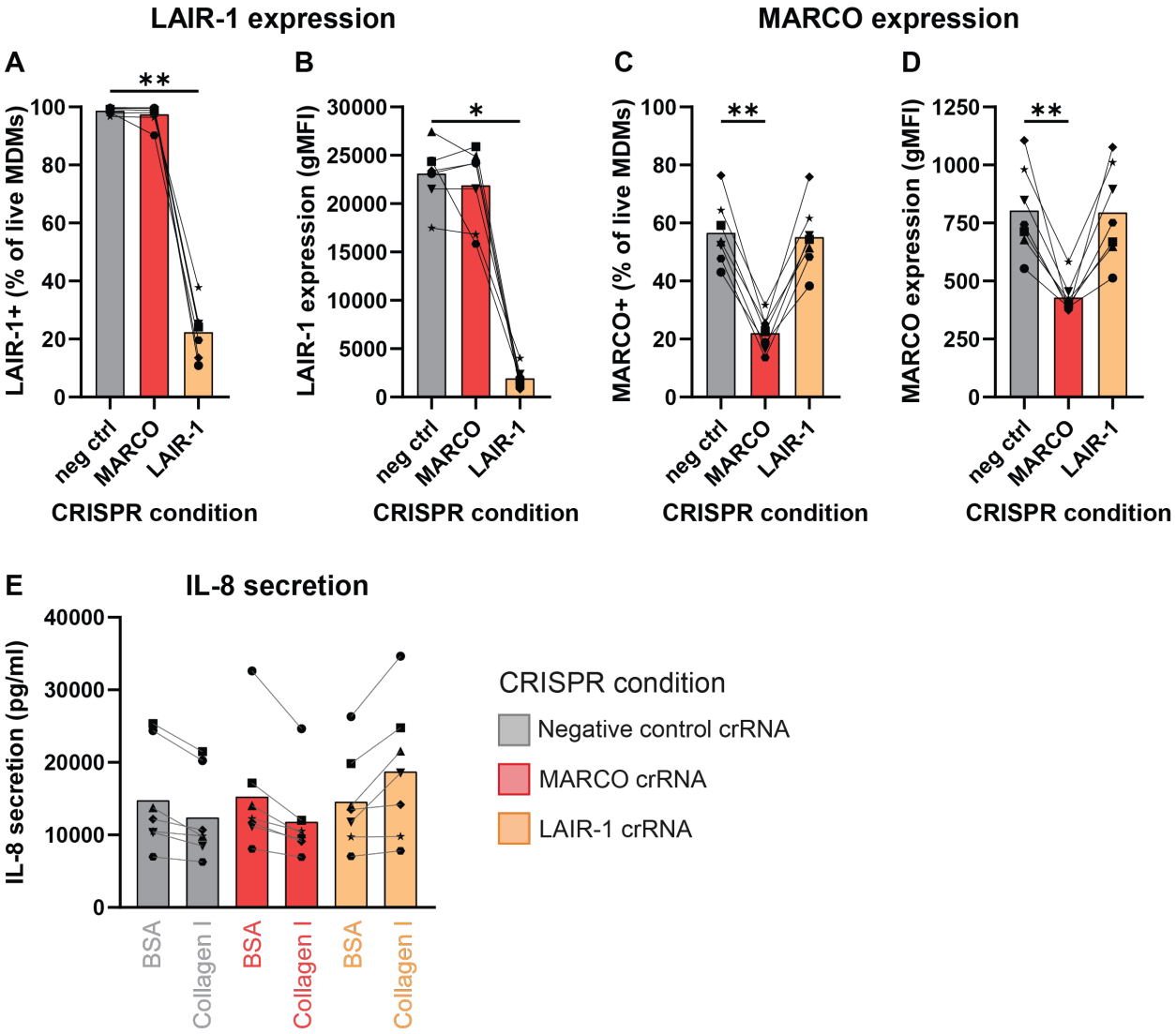

Fig. S3. Knockout efficiency of LAIR-1 and MARCO in primary human monocyte-derived macrophages and effects on IL-8 secretion. (**A** to **D**) Flow cytometric quantification of the expression of LAIR-1 (A and B) and MARCO (C and D) in human MDMs originating from monocytes treated by CRISPR/Cas9 to knockout the indicated targets. Data are from seven donors in three independent experiments and were analyzed by Friedman tests. *$P \leq 0.05$ and **$P \leq 0.01$. (**E**) The indicated MDMs incubated in BSA- or type I collagen–coated wells were stimulated with LPS, and the amounts of IL-8 that were secreted were quantified. The data shown are the raw data corresponding to the experiments shown in Fig. 5, C and D.